Angiogenic CD8 T cells from PWH induce Granzymes-dependent PAR1 activation promoting endothelial inflammation

Tong Li[1], Chinmayee Mehta[1], Cooper James[1], Jinya Chen[1], Hui Chen[1], Gerard P Ahern[2], Ziang Zhu[1], Maitane Faus Cid[1], Maryam Abdussamad[1], Shiwen Yu[1], Jai Kumar[3], Princy Kumar[3], Colleen Hadigan[4], Kyle DiVito[5], Dorian B McGavern[6], Leonid Pobezinsky[7], and Marta Catalfamo[1]

[1]Department of Microbiology and Immunology, Georgetown University School of Medicine. Washington DC, USA

[2]Department of Pharmacology and Physiology, Georgetown University School of Medicine. Washington DC, USA

[3]Division of Infectious Diseases and Travel Medicine, Georgetown University School of Medicine. Washington DC, USA

[4]Laboratory of Immunoregulation, National Institute of Allergy and Infectious Diseases, National Institutes of Health, Bethesda, MD 20892, USA

[5]Department of Biochemistry, Molecular and Cellular Biology, Georgetown University School of Medicine. Washington DC, USA

[6]Viral Immunology and Intravital Imaging Section, National Institute of Neurological Disorders and Stroke, National Institutes of Health, Bethesda, Maryland, USA

[7]Department of Veterinary and Animal Science, University of Massachusetts, Amherst, MA, USA

Abstract

In people with HIV (PWH), T cell immune activation and endothelial inflammation are contributors of the increased cardiovascular risk but the mechanisms remain poorly understood. In this study, we hypothesized that immune activation alters angiogenetic CD8 T cell (T_{ang}) function driving endothelial chronic inflammation. Endothelial cell repair is partially mediated by angiogenic T (T_{ang}) cells which facilitate proliferation and differentiation of bone marrow derived and resident endothelial progenitor cells at site of vascular injury. The role of CD8 T_{ang} cells in the setting of viral infection, including chronic HIV infection is largely unknown. In this study, we identified a subset of CD8 T cells expressing $CD31^{high}$ that exhibited a long-lived memory precursor phenotype ($CD127^{+}KLRG1^{-}$) and secreted the pro-angiogenic cytokine vascular endothelial growth factor (VEGF) in mice infected with acute LCMV. Furthermore, in PWH, the frequencies of circulating CD8 T_{ang} cells were reduced and showed an activated phenotype and expression of granzymes. $GZMA^{+}GZMB^{+}$CD8 T_{ang} cells correlated with atherosclerotic cardiovascular disease (ASCVD) risk. *In vitro*, granzyme dependent PAR1 activation led to calcium mobilization and secretion of pro-inflammatory cytokines IL-6, IL-8 and Angiopoietin-2 by primary human endothelial cells. Altogether, these findings suggest that HIV driven activation of CD8 T_{ang} cells promotes endothelial inflammation and chronic stimulation of this pathway may contribute to the increased risk of cardiovascular disease in PWH.

43 **Introduction**

44 Immune activation remains the hallmark of HIV infection, despite successfully suppressed
45 viremia by antiretroviral therapy (ART). HIV-associated inflammation and immune activation
46 drives cardiovascular risk, independent of traditional risk factors, duration of antiretroviral
47 treatment and CD4 counts (1-15). Compared to the general population, People with HIV (PWH)
48 have twice the risk of cardiovascular disease and standard cardiovascular risk prediction scores
49 underestimate cardiovascular risk in this population (16-18). The Strategic Timing of
50 AntiRetroviral Treatment (START) trial reported that the risk of AIDS and Serious non-AIDS
51 associated events (SNAEs) in early versus delayed treatment initiation was reduced, however,
52 excess risk remains for the most common non-AIDS defining illnesses, cardiovascular disease
53 (CVD) and cancer (19).

54 Atherosclerosis, the underlying pathology of cardiovascular events, is characterized by lipid
55 deposition, chronic inflammation, endothelial dysfunction; where cells from the innate and
56 adaptive immune system participate in the pathology of the disease (20). In PWH, CD8 T cell
57 immune activation is associated with carotid intima-media thickness and coronary plaque
58 suggesting an interplay between CD8 T cell activation and endothelial inflammation and
59 dysfunction (10, 11, 21-23). The molecular pathways by which HIV contributes to increased risk
60 of CVD remain largely unknown, which makes the development of more targeted therapies
61 difficult.

62 During systemic infections such as HIV, endothelial activation and injury can be mediated
63 by viral proteins and the host response (24, 25). Endothelial repair, is mediated in part by
64 angiogenic T cells (T_{ang}) that support proliferation and differentiation of bone marrow derived and
65 resident endothelial progenitor cells/endothelial colony forming cells (EPC/ECFC) at the site of

66 endothelial injury (26-28). In humans, T_{ang} cells have been defined by co-expression of CD31
67 (PECAM-1, Platelet endothelial cell adhesion molecule) and CXCR4 (stromal-cell-derived factor
68 receptor) (26). In addition, reduced circulating frequencies have been associated with age and
69 increased cardiovascular risk (26, 29, 30). However, their role in the setting of viral infections
70 including HIV has not been investigated.

71 Under physiological conditions, vascular permeability induced by trauma or infection triggers
72 activation of the coagulation cascade (leading to thrombin generation and clot formation) and a
73 host inflammatory response that promotes vascular and tissue repair. Thrombin, the main serine
74 protease of the coagulation cascade, connects the coagulation cascade, platelets and the host
75 inflammatory response by signaling through its receptor the Protease Activated Receptor 1 (PAR1)
76 expressed on immune cells. PAR1 is one of the four members of the seven transmembrane domain
77 G protein-coupled receptor family (PAR1, PAR2, PAR3 and PAR4) (31). PAR's activation is
78 mediated by proteolytic cleavage of the N-terminus that uncovers a tethered ligand (32, 33). In
79 humans, PAR1, PAR3 and PAR4 are activated by thrombin, whereas in mice PAR3 and PAR4 are
80 the main receptor for thrombin. In addition, PAR2 is activated by trypsin, tryptase and other
81 coagulation factors (32, 34-37).

82 CD8 T cells express PAR1, and its activation by thrombin enhances T cell function (32, 38-
83 41). These data provided evidence that PAR1 signaling mediates the cross-talk between the
84 coagulation system, endothelium and the adaptive immune system (CD8 T cells) at sites of
85 endothelial injury.

86 Thrombin-dependent activation of PAR1 occurs by proteolytic cleavage of the extracellular
87 domain at the Arg^{41}-Leu^{42} (32, 42, 43). In addition, other proteases including granzymes (A, B and
88 K) activate PAR1 although the cleavage site is not well defined. Moreover, granzyme-dependent

89 activation of PAR1 induces downstream signaling pathways that differ from thrombin leading to
90 a non-canonical activation or "biased signal" (43-50). Extracellular granzymes A, B and K have
91 been shown to induce inflammation by activating PAR1 in multiple cell types including neurons,
92 fibroblast and endothelial cells (44, 46-48, 50, 51).

93 In this study, we evaluated whether T_{ang} cells are involved in endothelial repair in response to
94 immune mediated injury during acute Lymphocytic Choriomeningitis virus (LCMV) infection.
95 We found that $CD31^{high}$ expressing CD8 T_{ang} cells increased after viral control, have a memory
96 precursor phenotype ($KLRG1^{-}CD127^{+}$) and secrete vascular endothelial growth factor (VEGF)
97 suggesting their contribution in endothelial repair. Moreover, we found that in the setting of
98 chronic HIV infection, immune activation drives a proinflammatory phenotype of CD8 T_{ang}
99 expressing granzymes. The frequencies of $GZMA^{+}GZMB^{+}$CD8 T_{ang} are associated with the
100 atherosclerotic cardiovascular disease (ASCVD) risk. In addition, plasma levels of GZMA
101 correlated with endothelial inflammatory markers including sVCAM1 and IL-6. *In vitro* GZMs
102 activate PAR1 favoring the secretion of pro-inflammatory cytokines over the pro-angiogenic
103 cytokines. This evidence supports the notion that HIV driven immune activation alters CD8 T_{ang}
104 cell function and chronic stimulation of this pathway may contribute endothelial inflammation and
105 the increased risk of cardiovascular disease.

106 **Material and Methods**

107 *Study Participants*

108 Participants were studied under a MedStar Georgetown University Hospital and NIAID
109 Institutional Review Board approved HIV clinical research studies. Characteristics of the study groups
110 of PWoH (n= 17) and PWH (n= 25) are described in Table 1. All study participants signed a written
111 informed consent for the collection of samples.

112

113 *C57BL/6 f2r$^{fl/fl}$ Mice*

114 The mouse carrying a conditional floxed (fl) PAR1 (C57BL/6 F2r$^{fl/fl}$) was constructed with
115 Ingenious Targeting Laboratories (NY, USA). Exon 2 of F2r gene was conditionally targeted and it is
116 fused in frame with p2A-Tomato reporter cassette. F2r and tdTomato genes are inactivated upon Cre
117 mediated deletion between the LoxP elements. A FRT/LoxP selection ivNeo marker as homology
118 arms were included in the final targeting vector.

119 Targeted iTL IN2 (C57BL/6) embryonic stem cells were microinjected into Balb/c blastocysts.
120 Resulting chimeras with a high percentage black coat color were mated to C57BL/6 FLP mice to
121 generate Somatic Neo Deleted mice. Confirmed somatic neomycin cassette deleted mice were bred
122 with wild-type C57BL/6N mice to generate germline neomycin cassette deleted floxed PAR1 mice
123 C57BL/6 f2r$^{fl/fl}$.

124 All mice were bred and maintained under specific pathogen-free conditions at Georgetown
125 University Division of Comparative Medicine facility. All experimental procedures were conducted
126 in accordance with the guidelines and an approved protocol by Institution Animal Care and Use
127 Committee at Georgetown University. Mice between 8 to 12 weeks old were used for experiments.

128

129 *RT-qPCR analysis*

130 qPCR was performed to determined mRNA expression of PARs in resting murine cells. RNA was
131 obtained from magnetic isolated B, CD4 and CD8 T cells (Miltenyi Biotech, MD). RNA was extracted
132 and purified using RNeasy Mini kit (Qiagen, MD). RNA was reverse transcribed into cDNA using
133 QuantiNova Reverse Transcription kit (Qiagen, Germany). qPCR performed with QuantiNova SYBR
134 Green PCR kit in CFX Opus Real-Time PCR system (Bio-Rad, CA). Primers used: murine *F2r*
135 (NM_010169.3): forward, 5′-ATGAAAGCGTCCTGCTGGAG-3′; reverse, 5′-
136 GGACGTTCAGAGGAAGGCTG-3′; murine *F2rl1* (NM_007974.4): forward, 5′-
137 GCTGGGAGGTATCACCCTTCT-3′; reverse, 5′-CGCAGAGAACTCATCGATGGA-3′; murine
138 *F2rl2* (NM_010170.4): forward, 5′-TGCCAGTCACTGTTTGCCAA-3′; reverse, 5′-
139 CTCGGGACACTCCGCTTTTAT-3′; murine *F2rl3* (NM_007975.3): forward, 5′-
140 GACCCCCAGCATCTACGATG-3′; reverse, 5′-CAGCAGCAGTGCTTGAGAGCT-3′.
141 Housekeeping gene HPRT was used: murine HPRT (NM_013556): forward, 5′ -
142 GCGATGATGAACCAGGTTATGA- 3′; reverse, 5′ - ACAATGTGATGGCCTCCCAT - 3′
143 LCMV Glycoprotein: forward, 5′- CATTCACCTGGACTTTGTCAGACTC -3′; reverse, 5′-
144 GCAACTGCTGTGTTCCCGAAA -3′ (52, 53).

145 Ct of each sample obtained from the amplification curve was normalized to HPRT
146 and calculated ΔCt (Ct gene of interest – Ct HPRT). Results were expressed as $2^{-\Delta Ct}$ value.

147

148 *LCMV infection*

149 C57BL/6-F2r$^{fl/fl}$ mice were intravenously infected with $2x10^5$ pfu LCMV Armstrong strain. At
150 days 6 and 21 post infection (p.i.), mice were anesthetized and perfused with cold HBSS before organs
151 (lung and spleen) were collected. *In vivo* CD8 T cell depletion was performed in LCMV infected mice

152 at day 15 p.i.. Mice were administered (i.p.) with 300 μg of anti-mouse CD8α mAbs (YTS 169.4,
153 BioCell, MA) or IgG2b isotype control (LTF-2, BioCell, MA). CD8 T cell depletion was confirmed
154 by flow cytometry in lung and spleen.

155 Cell suspensions from the spleens were obtained by smashing the spleens with a syringe plunger
156 in PBS and red blood cells were lysed with ACK (Gibco, MA) for 3 min on ice. After cell lysis cell
157 suspension was passed through a 70 μm mesh, and cell count and viability was assessed.

158 Cell suspension from the lungs were obtained by enzymatic digestion. Lungs were cut into small
159 pieces and digested using Lung Dissociation kit (Miltenyi Biotech, MD). The total cell suspensions
160 were passed through a 70 μm mesh, and cell count and viability were assessed. The total cell
161 suspension was used to analyze endothelial cells in the lung. For T cell analysis immune cell
162 enrichment was performed using 35% Percoll gradient. Total lung cell suspensions were centrifuged
163 and the pellet resuspended in 12 ml of 35% Percoll (Sigma, MA) and centrifuged for 15 min without
164 break at 1800 rpm (757g) at 7 °C. Immune cell suspensions were passed through a 70 μm mesh, and
165 cell count and viability were assessed.

166

167 *Flow cytometry:*

168 *Phenotype lymph organs and endothelial cell phenotype*: $2x10^6$ of cells from spleen, lymph nodes
169 and lung cells (pre-Percoll) were stained with LIVE/DEAD (Invitrogen, CA) for 30 minutes at 4ºC.
170 Cells were incubated with a cocktail of mAbs (Table S1, panel-1 and panel-2) for 20 minutes at 4ºC.
171 Cell were washed with staining buffer (HBSS with 0.01% of NaN_3 and 0.01% of BSA) twice and
172 acquired with a BD Symphony (BD Biosciences, CA). Cells were analyzed with FlowJo (BD
173 Biosciences, CA).

174 *Cytokine secretion assay*: $2x10^6$ splenic and immune lung cells (post-Percoll) were stimulated *in*
175 *vitro* with 1 μg/mL of LCMVGp33-41 peptide (KAVYNFATC, Anaspec, CA) in the presence of 5
176 μg/mL of Brefeldin A (Sigma, MA) and 50 U/mL of rhIL-2 (National Cancer Institution, MD) for 4
177 hours at 37°C and 5% CO_2. After stimulation, cells were stained with LIVE/DEAD (Invitrogen, CA)
178 for 30 minutes at 4ºC. Cells were washed twice and incubated with surface mAbs cocktail (Table S1,
179 panel-3) for 20 min at 4ºC. Cells were fixed and permeabilized with BD Cytofix/Cytoperm solution
180 (BD Bioscience, CA) and incubated with the mAbs cocktail for intracellular markers for 20 min at
181 4ºC (Table S2 panel-2). Samples were acquired in a BD Symphony and analyzed with FlowJo (BD
182 Biosciences, CA).

183 *MHC class I pentamer staining*: $1x10^6$ splenic and lung immune cells from infected mice were
184 stained with H-$2D^b$ restricted LCMVGP33-41aa pentamer (H-$2D^b$-KAVYNFATC, Proimmune, UK)
185 at room temperature (22 ºC) for 10 min followed by incubation with surface mAbs cocktail (Table S1)
186 for 20 min at 4ºC. Cell suspensions were acquired in a BD Symphony (BD Biosciences, CA) and
187 analyzed using FlowJo.

188 *CD8 T_{ang} sorting and cytokine secretion*: T cells were isolated from the lungs as described above.
189 Lung cell suspensions from naïve and infected mice at day 21 p.i. were stained with a cocktail of mAbs
190 for 20 minutes at 4ºC (Table S1) and live cells were selected using Sytox Blue staining before sorting
191 (Biolegend, CA). $CD31^{high}$ and $CD31^{neg}$ CD8 T cells were sorted on a FACSAria (BD Bioscience,
192 CA). T cells were stimulated at a concentration of 300,000 cells/mL in plates with cross-linked anti-
193 CD3 and anti-CD28 mAbs (BD Bioscience, CA). After 3 days of culture, supernatants were collected
194 and cytokines (M-CSF, PDGF-A, GM-CSF, IL-2, IL-4, IL-5, IL-13, IL-17A, IL-6, IL-22, IL-9 and
195 IL-10) were measured using LEGENDplex (Biolegend, CA) following manufacturer's instructions.
196 Briefly, 25 μL of sample in duplicates were incubated with capture mAbs coated beads for 2 hours

197 followed by incubation with detection mAbs for 1 hour at room temperature in a shaker. Each sample
198 was incubated with streptavidin-PE for 30 min and acquired with a BD Symphony (BD Biosciences,
199 CA). Results were analyzed using cloud-based software Qognit (Qognit Inc, CA).

200 *Flow cytometry human peripheral blood mononuclear cells*

201 Whole blood from PWoH (n= 17) and PWH (n= 25) were collected in BD Vacutainer blood
202 collection tube containing EDTA (BD Bioscience, CA). Whole blood was diluted with PBS with 2%
203 FBS (1:1) and loaded on the top of Ficoll-Paque (Cytiva, MA) followed by a centrifugation at 400xg
204 for 30 min at room temperature (25°C). Peripheral blood mononuclear cells (PBMCs) were collected
205 and stained with LIVE/DEAD (Invitrogen, CA) for 30 minutes at 4ºC. Cells were incubated with
206 1μg/mL human IgG (Sigma, MO) for 10 minutes at 4ºC to block Fc receptors followed by incubation
207 with a monoclonal antibodies (mAbs) cocktail (Table S2, panel-1) for 30 minutes at 4ºC. Samples
208 were acquired with a BD Symphony (BD Biosciences, CA) and analyzed using FlowJo software.

209 *Measurements of cytokines and biomarkers of endothelial inflammation in plasma*

210 Plasma were obtained from whole blood collected in BD Vacutainer blood collection tube
211 containing EDTA (BD Bioscience, CA) from PWH (n= 25) and stored at -80°C until use. Cytokines,
212 biomarkers of endothelial inflammation and granzymes (VCAM-1, IL-6, TNFα, IFNγ, sFasL, IL-2,
213 granzyme A and granzyme B) were measured using LEGENDplex (Biolegend, CA) following
214 manufacturer's instructions as described above.

215 *Unsupervised clustering analysis*

216 Multidimensional analysis was performed using Phenograph algorithm (FlowJo, CA). 10,000 of
217 manually gated lung endothelial cells ($CD326^{-}CD45^{-}CD31^{+}$) were concatenated from naïve mice and
218 infected mice at days 6 and 21 p.i.. Samples acquired in different days were normalized using Mutual
219 Nearest Neighbors (MNN) (FlowJo, CA) (54). Unsupervised clusters were analyzed with Phenograph

220 (k= 100) based on surface markers (CD31, PDL1, tdTomato, CD34, CD309, VCAM-1, CD105,
221 CD90.2 and CD201). Mean fluorescence intensity of each marker for all the clusters was presented in
222 heatmap and median frequency of each cluster from naïve and infected mice were expressed as bubble
223 plots.
224
225 *Co-culture of primary human umbilical vein endothelial cells (HUVEC) and CD8 T_{ang} cells*
226 Frozen PBMCs from PWoH (n= 10) and PWH (n= 10) were thawed and rested for 2 hours. Cells
227 were incubated with 1μg/mL human IgG (Sigma, MO) for 10 minutes at 4ºC to block Fc receptors
228 followed by a cocktail of mAbs incubation for 30 minutes at 4ºC (Table S2, panel-2). Live cells were
229 selected using Sytox Blue staining before sorting (Biolegend, CA). CD8 T_{ang} cells were sorted on a
230 FACSAria (BD, CA) and centrifuged at 1000 rpm for 30 minutes. Sorted CD8 T_{ang} cells were activated
231 with anti-CD3 and anti-CD28 mAbs coated beads (Miltenyi Biotech, MD) for 3 days and expanded in
232 the presence of 50 U/mL of recombinant human (rh) IL-2 (National Cancer Institution, MD) for 14
233 days. 5,000 HUVEC and 100,000 of CD8 T_{ang} cells were resuspended in endothelial cell growth basal
234 media (Lonza, CA) and seeded in the 96 well plate in the presence or absence of anti-CD3/anti-CD28
235 mAbs coated beads (Miltenyi Biotech, MD) and incubated at 37ºC and 5% CO_2 overnight. As a
236 control, HUVEC alone was stimulated with 20 ng/mL of rhIFNγ (PeproTech, NJ) and 0.5 ng/mL of
237 rhTNFα (R&D System, MN) overnight. Cytokines in supernatant were measured using LEGENDplex
238 (Biolegend, CA) as described above.
239
240 *Tube formation assay*
241 Frozen PBMCs from PWH (n= 3) and PWoH (n= 2) were thawed and rested for 2 hours and sorted
242 as described above. Cells were incubated with 1μg/mL human IgG (Sigma, MO) for 10 minutes at

243 4ºC to block Fc receptors followed by a cocktail of mAbs incubation for 30 minutes at 4ºC (Table S2,
244 panel 2). Live cells were selected using Sytox Blue staining before sorting (Biolegend, CA). CD8 T_{ang}
245 memory cells ($CD45RA^{-}CD27^{+}$) were sorted as described above. For HIV-Gag-specific CD8 T cells,
246 PBMCs from PWH were stimulated with HIV_{gag} peptide pool (2 μg/mL, NIH AIDS Reagent Program)
247 overnight and $CD137^{+}$CD8 T cells were sorted. Sorted cells were washed twice with cold PBS and
248 labeled with 1.5 μM of CSFE (Invitrogen, CA) for 8 min at 37 ºC followed by quenching with cold
249 FBS for 5 min on ice. CFSE labeled sorted cells were rested overnight. 10 μL of basement membrane
250 extract (Cultrex reduced growth factor, R&D System, MN) was applied in the inner well of 15 well
251 μ-slide chambered coverslip (ibidi, WI) and incubated for 20 min at 37°C for gelation. HUVEC and
252 CFSE labeled CD8 T_{ang} cells were resuspend in endothelial cell growth basal media (Lonza, CA) at
253 2:1 endothelial cell to T cell ratio and seeded on the top of gel in each well. Chambered coverslips
254 (Ibidi, WI) were incubated in a stage-top cell incubator at 37°C and 5% CO_2 and evaluated using Leica
255 SP8 live cell imaging (Leica, IL) at 4, 6, 8, 10 and 12 hours at 10X magnification. Analysis was
256 analyzed using image analysis platform Wimasis (Wimasis GmbH, Germany).
257
258 *Calcium mobilization assay*
259 60,000 HUVEC were cultured on a coverslip in endothelial cell growth media (Lonza, CA) for 8
260 hours and starved with endothelial cell growth basal media-2 (EBM-2) containing 1% PBS overnight.
261 Cells were loaded for 40 min with 1 μM Fluo-4-AM (Invitrogen, Thermo Fisher Scientific) in a buffer
262 solution containing 140 mM NaCl, 4 mM KCl, 1 mM $MgCl_2$, 1.2 mM $CaCl_2$, 10 mM HEPES, and 5
263 mM glucose (pH 7.3). Cells were imaged with 20X objective using a Nikon TE2000 microscope with
264 an excitation filter of 480 ± 15 nm and an emission filter of 535 ± 25 nm. The images were captured
265 by a Retiga 3000 digital camera (QImaging) and analysis was performed offline using ImageJ.

266 *Granzyme- dependent PAR1 activation*

267 100,000 HUVEC were seeded a 12 well plate in endothelial cell growth media supplemented with
268 EGM-2 bullet kit overnight. Next day cells were starved in EBM-2 containing 1% FBS for 6 hours.
269 HUVEC were incubated pre-incubated with 10 μg/mL of ATAP-2 (Invitrogen, CA) or 300 nM of
270 PAR1 antagonist SCH530348 diluted in EBM-2 containing 1% FBS for 20 min at room temperature
271 (25°C). After the preincubation period, supernatants were removed from the wells, and HUVEC were
272 stimulated with 100 nM of recombinant human granzyme A (rhGZMA, Kamiya Biomedical, WA)
273 and recombinant human granzyme K (rhGZMK, Kamiya Biomedical, Japan) with fresh inhibitors at
274 the same concentration. As the positive control, HUVEC were incubated with 100 μM of PAR1
275 agonist TFLLR-NH2 (Tocris Bioscience, UK) and control peptide RLLFT-NH2 (Tocris Bioscience,
276 UK). After overnight incubation at 37°C and 5% CO_2 supernatants were collected and cytokines were
277 measured using LEGENDplex (Biolegend, CA) as described above.

278

279 *Statistical analysis*

280 Comparisons were performed using non-parametric Mann-Whitney test or Wilcoxon test and
281 p value $\leqslant$ 0.05 was considered significant. Correlations were performed using nonparametric
282 Spearman correlation and p value $\leqslant$ 0.01 was considered significant.

283

284 **Results**

285 **PAR1 expression is modulated in virus-specific CD8 T lymphocytes during acute LCMV**
286 **infection**

287 At the site of vascular injury mediated by trauma or infection, the cross-talk between the
288 coagulation cascade, platelets, endothelial cells and CD8 T cells is mediated by thrombin
289 dependent activation of PAR1 (32, 38, 40, 55). Particularly, PAR1 signaling is involved in CD8 T
290 cell trafficking and function (40, 41). However, whether PAR1 is modulated in CD8 T cells
291 during the immune response remains to be defined.

292 We generated a PAR1 reporter mouse that allows us to evaluate PAR1 expression in CD8 T
293 cells during the course of a systemic viral infection and better understand the interplay between
294 CD8 T cells and endothelial cells. C57BL/6 F2r$^{fl/fl}$ mouse carrying floxed Exon 2 of *F2r* gene was
295 conditionally targeted as well as fused in frame with p2A-Tomato (tdT) reporter cassette (as
296 described in Material and Methods section and Figure S1A).

297 C57BL/6 F2r$^{fl/fl}$ mice showed similar cell numbers in lymph nodes and spleen compared with
298 the wild type C57BL/6 (Figure S1B). The frequencies and cell count of innate cells including
299 neutrophils, eosinophils, monocytes, macrophages and dendritic cell subsets were similar between
300 the C57BL/6 F2r$^{fl/fl}$ and the C57BL/6 wild type mice (Figure S1C and D). Similarly, no significant
301 differences between C57BL/6 F2r$^{fl/fl}$ and wild type mice were observed in the frequencies and cell
302 numbers of lymphocytes subsets, B, NK and T cells in lymphoid organs (Figure S1E).

303 PAR1 expression, tdTomato^{+} (tdT^{+}) cells, included CD4 and CD8 T cells and NK cells and it
304 was negligible in B cells (Figure 1A, B and C). Similar to our previous observations in human T
305 cells, CD8 T cells expressed higher levels of PAR1 compared with CD4 T cells. Among
306 lymphocytes, NK expressed the highest level of PAR1 at steady state conditions (Figure 1C) (41).

307 mRNA of *F2r* expression in tdT expressing cells was further confirmed by qPCR in magnetic
308 cell isolated CD4 and CD8 T cells and B cells. CD8 T cells expressed higher levels of mRNA of
309 *F2r* than CD4 T cells (Figure 1D). In addition, both CD4 and CD8 T cells expressed mRNA *F2rl1*
310 (PAR2) but not *F2rL2* (PAR3) and *F2rl3* (PAR4) (data not shown)(41). PAR1 protein expression
311 in CD4 and CD8 T cells was further confirmed by flow cytometry in tdT^+ T cells (Figure S2).
312 These data show that at steady state conditions, PAR1 is expressed in T and NK but not B
313 lymphocytes.

314 We next investigated the expression of PAR1 in virus-specific CD8 T cells during a systemic
315 acute viral infection with the Lymphocytic Choriomeningitis virus Armstrong strain (LCMVArm).
316 This infection model recapitulates features of human viral infections, the acute form, LCMV
317 Armstrong (Arm) is cleared 8-10 days post infection (p.i) and induces the generation of LCMV-
318 specific memory CD8 T cells (56-58). LCMV is a non-cytolytic virus and the pathology induced
319 is mediated by the host immune response (59, 60).

320 Using this model, we aimed to determine the immune mediated endothelial injury in the lung,
321 and address whether T cells are involved in endothelial repair after viral control. We studied two
322 time points of the LCMVArm infection, day 6 p.i (effector phase) and day 21 p.i (contraction phase
323 and early memory development) (58, 61).

324 LCMVGp33-specific CD8 T cells secreted IFNγ, TNFα and showed cytotoxic potential (as
325 measured by CD107a surface expression) upon *in vitro* stimulation with LCMVGp33-41aa peptide
326 (Figure S3A and B). LCMVGp33-specific CD8 T cells peaked by day 6 p.i in both spleen and
327 lung and declined by day 21 in the spleen when the virus is controlled (Figure S3A and B). In
328 contrast, in the lung, LCMVGp33-specific CD8 T cells remain higher consistent with development
329 of memory cells (Figure S3A and B).

330 Expression of PAR1 was monitored by tdT^+ cells in total CD8 T cells and virus-specific CD8
331 T cells using pentamer staining (H2-D^bLCMVGp33-41aa) (Figure S3C and Figure 1E
332 respectively). At day 6 p.i. and compared to total CD8 T cells from the naïve (dashed line) mice,
333 expression of PAR1 (tdT^+) in LCMVGp33-specific CD8 T cells was reduced, and it was
334 significantly upregulated by day 21 p.i. (Figure 1E and F). Similar observations were noted in total
335 CD8 T cells in both spleen and lung (Figure S3C). PAR1 transcriptional regulation in
336 LCMVGp33-specific CD8 T cells may be induced by *in vivo* granzyme activation during
337 degranulation (Figure S3B) (41). Accordantly, tdT expression by $CD107a^+$CD8 T cells showed
338 lower expression of granzyme A compared to $CD107a^-$CD8 T cells (Figure S3D and E). In
339 addition, tdT^+CD8 T cells negatively correlated with the frequency of $GZMA^+$CD8 T cells, R= -
340 0.61, p= 0.02.
341 Altogether these data show that PAR1 is expressed at distinct stages of CD8 T cell
342 differentiation. *In vivo*, PAR1 expression is downregulated at the effector phase and upregulated
343 after viral control and memory development.
344
345 **Angiogenic $CD31^{high}$CD8 T (T_{ang}) cells promote endothelial recovery during acute viral**
346 **infection**
347 T_{ang} cells have been originally described in the center of the endothelial progenitor cell colonies
348 isolated from peripheral mononuclear cells (PBMCs). In *in vivo* experiments, T_{ang} cells support
349 new vessel formation (26). However, whether T_{ang} cells are virus-specific CD8 T cells that acquire
350 these properties once the infection is controlled and are involved in endothelial repair remains
351 poorly understood.

352 We hypothesized that systemic LCMVArm infection induces immune mediated endothelial
353 injury in the lung, and T_{ang} cells play a role in repair after viral control. We found that at day 6 p.i.,
354 when LCMV-specific CD8 T cells are recruited into the lung, there was a significant reduction in
355 the frequency and cell count of lung endothelial cells (ECs) (Figure 1G). ECs recovered to baseline
356 levels by day 21 p.i. (Figure 1G). In contrast to CD8 T cells, expression of PAR1 in endothelial
357 cells increased over the course of infection suggesting that PAR1 can be targeted by different
358 proteases during the course of the infection (Figure 1H). These data show that immune mediated
359 endothelial cell injury occurs in lung during a systemic viral infection and recovers upon viral
360 control.

361 We next determined if CD8 T cells are involved in the recovery of lung ECs. LCMV infected
362 mice were either treated with anti-CD8 mAb and IgG control at day 15 p.i. when the infection is
363 controlled. CD8 T cells were efficiently depleted in the lung by day 21 p.i. (Figure 2A). Compared
364 to the mice treated with IgG control, CD8 T cell depleted mice showed a delayed recovery of EC
365 count suggesting that CD8 T cells are involved in this process (Figure 2B). At this time point of
366 infection, we did not detect LCMV Glycoprotein by qPCR in both spleen and lung suggesting viral
367 control (Figure S4A) (62).

368 We next tested the hypothesis that the delayed recovery of lung ECs is associated with the loss
369 of CD8 T_{ang} cells during depletion. T_{ang} cells have been defined by expression of CD31 (26). In
370 the lung, during the course of the LCMV infection, a small subset of CD8 T cells expressed
371 $CD31^{high}$ and CD309 (vascular endothelial growth factor receptor 2 (VEGFR2)) and although the
372 frequency showed an increased trend by day 21 p.i., did not rich statistical significance (Figure
373 2C). In contrast, $CD31^{high}$CD8 T cell count was significant increased suggesting an expansion of
374 this subset during the recovery phase of lung ECs (Figure 2C). The expression of PAR1 of the

375 CD31^{high} and CD31^{low} CD8 T cells followed the similar kinetics to that observed in LCMVGp33-
376 specific CD8 T cells (Figure S4B and Figure 1F).
377 We then investigated whether CD31^{high}CD8 T cells were LCMV-specific and secrete
378 cytokines upon *in vitro* stimulation with LCMVGp33 peptide (Figure 2D). At day 21 p.i. and
379 compared to CD31^{neg}CD8 T cells, CD31^{high}CD8 T_{ang} cells secrete similar levels of IFNγ, TNFα
380 and have similar cytotoxic potential (CD107a). Of note, the frequency of CD31^{high}LCMVGp33-
381 specific CD8 T cells single IFNγ producers were reduced compared to the CD31^{neg} (Figure 3D).
382 Interestingly, LCMVGp33-specific CD31^{high}CD8 T cells were enriched in the memory
383 precursor effector T cells (KLRG1^{-}CD127^{+}), which have survival advantage during the
384 contraction phase and possesses plasticity to give rise to multiple memory subsets (Figure 2E)
385 (63-66). As expected, at day 21 p.i., a reduction of double positive effectors (KLRG1^{+}CD127^{+})
386 and short-live effector KLRG1^{+}CD127^{-} and KLRG1^{-}CD127^{-} CD8 T cells was observed at day
387 21 p.i. (Figure 2E).
388 In addition, we evaluated the ability of lung CD31^{high}CD8 T cells to secrete pro-angiogenic
389 cytokines and T cell helper cytokines. We sorted CD31^{high} and CD31^{neg} bulk CD8 T cells from
390 lung of LCMV mice infected at day 21 p.i., and CD31^{high} bulk CD8 T cells from lung of naïve
391 mice as control. Sorted subsets were TCR stimulated with cross-linked CD3 and CD28 mAbs for
392 3 days and cytokines were measured in the supernatants (Figure 2F and Figure S4C). CD31^{high}
393 but not CD31^{neg}CD8 T cells secreted vascular endothelial growth factor (VEGF), a cytokine that
394 induces proliferation of ECs suggesting a pro-angiogenic function (67, 68). In addition, compared
395 to the CD31^{neg}, CD31^{high}CD8 T cells showed an increased trend, although not significant, in the
396 ability to secrete granulocyte-macrophage-colony stimulating factor (GM-CSF), known to induce
397 EC proliferation and mobilize endothelial progenitor cells from the bone marrow (Figure S4C)

398 (69, 70). Lastly, CD31^{high}CD8 T cells showed the ability to secrete of IL-2 and secrete low levels
399 of Th2, Th17, Th22 and Th9 associated cytokines (Figure S4C).
400 These data suggest that angiogenic CD31^{high}CD8 T_{ang} cells are virus specific with an enriched
401 memory precursor phenotype. In addition, CD31^{high}CD8 T_{ang} secrete pro-angiogenic cytokines
402 contributing to lung EC recovery after viral control.
403
404 **Endothelial recovery is associated to CD31^{high}CD8 T_{ang} cells**
405 We next investigated the relationships between CD8 T_{ang} cells and lung ECs during the course
406 of the LCMV infection. ECs are heterogenous and play important roles by supporting immune cell
407 trafficking and regulating inflammation during immunity (71-73). Diverse phenotypes with
408 distinct functions including "immune cell-like" and "developmental/regenerative" involved in
409 immunity and repair respectively have been described (74, 75).
410 We hypothesized that during the expansion of CD31^{high}CD8 T_{ang} cells and recovery EC phase
411 ECs will be enriched with a regenerative phenotype. We determined the expression of markers
412 associated with inflammation (PD-L1, VCAM1) and pro-angiogenic/repair (CD34, CD309,
413 CD105) (60, 74, 76, 77). CD309 is a receptor for the VEGF, an essential factor for EC function
414 during angiogenesis (67). CD105 (Endoglin) binds to different components of the TGF-β
415 superfamily and also regulates endothelial proliferation, migration, and vascular homeostasis (78,
416 79). In addition, CD90.2 was used as maker for lymphatic endothelial cells (80).
417 We performed an unsupervised cluster analysis using PhenoGraph to classify high-parameter
418 single-cell data into phenotypically distinct clusters (81). We concatenated 10,000 events per
419 mouse of CD326^{-}CD45^{-}CD31^{+} lung ECs from Naïve and LCMV infected mice from day 6 and 21
420 p.i. to analyze the dynamics of endothelial cells (Figure 3A).

421 We found that the frequency of lung EC clusters (CL) 1, 2, 3, and small CL 7, and 8
422 significantly increased at day 6.p.i (Figure 3A, bubble plots and Figure S5). These CLs expressed
423 higher levels of PD-L1 and distinct levels of CD31 and PAR1 (Figure 3A). Expression of PD-L1
424 suggest that endothelial cells interact with immune cells modulating immune mediated pathology
425 through PD1-PD-L1 interaction (82).

426 The CL4, 5, 6, and 13 were present in the naïve mice and at day 21 p.i. (Figure 3A and Figure
427 S5). These clusters expressed markers associated with EC proliferation including CD105
428 (Endoglin), and CD309 (VEGFR2), A small EC subset (CL14), expressed high levels of CD105
429 and was expanded by day 21 p.i. suggesting a "regenerative" phenotype (Figure S5). In addition,
430 CL10 and CL11 remained significantly reduced compared to the naïve mice. CL9 correspond to
431 CD90.2^{+} lymphatic endothelial cells and its frequency remained constant through the course of the
432 infection.

433 These data suggested that ECs are heterogenous and dynamic during viral infection. The ECs
434 in CL6 expressed CD201 (endothelial protein C receptor, EPCR), a marker associated with
435 resident vascular endothelial cell progenitors and activated protein C (APC) dependent activation
436 of PAR1 during angiogenesis (75, 83, 84). More importantly, CL6 expressed higher levels of
437 CD105, CD309 and CD34 suggesting a proliferative and regenerative phenotype (76).

438 Interestingly, CL6 was positively associated (R= 0.66, p< 0.01) with the frequency of
439 CD31^{high}CD8 T_{ang} cells suggesting potential interaction during vascular remodeling (Figure 3B).
440 Altogether these data suggest that CD31^{high}CD8 T_{ang} cells play a role in endothelial remodeling
441 during infection.

442

443 **Circulating angiogenic CD8 T (T_{ang}) cells from PWH have pro-inflammatory phenotype.**

444 The data above shows that during a systemic viral infection the host immune response mediates
445 endothelial injury and CD31^{high}CD8 T_{ang} cells play a role in endothelial repair by secreting pro-
446 angiogenic cytokines involved in endothelial proliferation and remodeling.

447 The role of T_{ang} cells in the setting of human chronic viral infections such as HIV remains to
448 be defined. Previously, we reported that circulating T_{ang} cells from PWH express the vascular
449 homing receptor CX3CR1 suggesting their recruitment to the sites of endothelial inflammation
450 (85). Given that immune activation and systemic inflammation are the main features of chronic
451 HIV infection, we hypothesized that this environment alters T_{ang} cell function promoting a pro-
452 inflammatory function that contributes to endothelial inflammation.

453 To address this question, we investigated circulating T_{ang} cells in PBMCs from PWH (n= 25)
454 and uninfected controls People without HIV (PWoH, n=17). PWH had a median CD4 count 663
455 (532-861.5) cells/μL and HIV RNA viral load < 20 copies/mL (n= 20) and 50-110 copies/mL (n=
456 4). Study participants had a median ASCVD (Atherosclerosis Cardiovascular Disease) risk score
457 of 7.9 (IQR: 5.0-18.6) (Table 1).

458 In humans, T_{ang} cells are defined as surface expression of CD31/PECAM-1 (Platelet
459 Endothelial Cell Adhesion Molecule) and the chemokine receptor CXCR4 (receptor for the
460 Stromal Cell Derived Factor-1) *(26, 86)*. The flow cytometry analysis showed that in PWH there
461 is a significantly reduction in the frequencies of circulating CD8 T_{ang} cells (p< 0.001). A trend
462 although not statistically significant was observed in CD4 T_{ang} cells as well (Figure 4A and B).

463 To evaluate the impact of HIV driven immune activation, we studied expression of markers
464 associated with adhesion, homing and trafficking during vascular inflammation including the
465 Protease Activated Receptor 1 (PAR1) which is involved in the recruitment of T cells at the site
466 of vascular injury (38, 40, 41). In addition, we investigated the vascular homing receptor CX3CR1

467 that binds to CX3CL1 (fractalkine) expressed by inflamed endothelial cells, and the integrin
468 CD49f (Integrin alpha-6) that binds to laminin, a component of the vascular basement membrane
469 (38-40, 87).

470 In PWH, both CD4 T_{ang} and CD8 T_{ang} cells showed significantly increased expression of
471 PAR1, CX3CR1 and CD49f compared to PWoH suggesting an increased potential for recruitment
472 and trafficking to the sites of vascular inflammation (Figure 4C and D). In addition to the increased
473 trafficking potential, both CD4 T_{ang} and CD8 T_{ang} cells from PWH showed an increased expression
474 of effector molecules Granzyme A (GZMA) and Granzyme B (GZMB) when compared to PWoH
475 (Figure 4E).

476 All together these data suggest that PWH and virally suppressed by ART have a significant
477 reduction in the frequencies of CD8 but not CD4 T_{ang} cells. T_{ang} cells showed a differentiated
478 phenotype with cytotoxic potential and increased potential to migrate to the sites of vascular
479 inflammation.

480

481 **Frequencies of activated CD8 T_{ang} cells are associated with cardiovascular risk in PWH**

482 In PWH, immune activation, systemic inflammation and endothelial dysfunction have been
483 identified as the main drivers of cardiovascular events (4, 9-11, 88). The data above suggest that
484 in the context of HIV infection T_{ang} cells have a pro-inflammatory phenotype. We next investigated
485 the relationship between activation markers expressed by T_{ang} cells and the Atherosclerotic
486 Cardiovascular Disease (ASCVD) risk score (Figure 4F, G and H).

487 The frequencies of circulating total CD4 and CD8 T_{ang} cells did not show an association with
488 ASCVD (data not shown). In contrast, we observed a positive correlation between ASCVD and
489 the frequency of cells expressing activation markers including homing and trafficking

490 CX3CR1$^+$PAR1$^+$CD8 T_{ang} and CD49f$^+$PAR1$^+$CD8 T_{ang} (R= 0.50, *p*= 0.04 and R= 0.58, *p*= 0.02
491 respectively) (Figure 4F and G). Similarly, GZMA$^+$GZMB$^+$CD8 T_{ang} cells showed a positive
492 association with the ASCVD risk score R= 0.65, *p*< 0.01 (Figure 4H). Of note is that expression
493 of these markers in CD4 T_{angs} cells did not correlate with ASCVD risk (Figure 4F, G and H). These
494 observations suggest that in PWH immune activation of CD8 T_{ang} cells drives a pro-inflammatory
495 phenotype and may play a role in sustaining endothelial inflammation.

496 To better address the potential contribution of activated CD8 T_{ang} cells on endothelial
497 inflammation, we further studied the relationship between plasma levels of biomarkers of
498 endothelial inflammation and immune cell trafficking including soluble Vascular and Intracellular
499 Adhesion Molecule-1 (sVCAM-1 and sICAM-1 respectively), IL-6; and T cell-derived cytokines
500 and effector molecules including TNFα, IFNγ, IL-2, sFASL, GZMA and GZMB (Figure 4I and
501 Figure S6A). We found that plasma levels of GZMA but not GZMB were positively associated
502 with IL-6 (R= 0.62, p< 0.001). sVCAM-1 showed a positive trend (R= 0.449, *p*= 0.024) but not
503 with sICAM-1 (Figure 4I). As expected, plasma levels of cytokines (TNFα, IFNγ, sFASL, IL-2)
504 positively correlated with the plasma levels of granzymes (Figure S6A).

505 Altogether the data shows that chronic HIV driven immune activation increase trafficking and
506 pro-inflammatory properties of CD8 T_{ang} cells. Moreover, the association with ASCVD suggest
507 that CD8 T_{ang} cells may contribute to endothelial inflammation, dysfunction and disease risk.

508

509 ***In vitro,* CD8 T_{ang} cells from PWH showed enhanced ability to induced sICAM-1 and**
510 **VCAM-1 by endothelial cells.**

511 The above results suggest that chronic HIV infection alters CD8 T_{ang} cells skewing their
512 function to pro-inflammatory. Because activated CD8 but not CD4 T_{ang} cells showed association

513 with cardiovascular risk in the following sections of the manuscript we focused our study on CD8
514 T_{ang} cells.

515 To address the potential mechanisms involved by which CD8 T_{ang} cells drive endothelial
516 inflammation, we first determined the effects of *in vitro* activated CD8 T_{ang} cells on primary
517 Human Umbilical Vein Endothelial cells (HUVEC). In the supernatants of the co-cultures, we
518 measured adhesion molecules including sICAM-1 and sVCAM-1, pro-inflammatory cytokines IL-
519 6, Angiopoetin-2 (Ang-2) and IL-8; and pro-angiogenic cytokines, basic Fibroblast Growth Factor
520 (bFGF) and Vascular Endothelial Growth Factors (VEGF) (89-91).

521 CD8 T_{ang} cells from PWH (n= 10) and PWoH (n= 10) were sorted based on the expression of
522 CD31, CXCR4 and memory phenotype. CD8 T_{ang} cells were *in vitro* expanded with anti-
523 CD3/CD28 mAbs and rhIL-2 (50 U/ml) for 14 days. Expanded CD8 T_{ang} cells were co-cultured
524 with HUVEC at 20:1 CD8 T_{ang} to HUVEC ratio and stimulated in media (control) and with anti-
525 CD3/CD28 mAbs coated beads overnight.

526 CD8 T_{ang} co-cultured with HUVEC cells in media alone showed negligible levels of shedding
527 of sICAM-1 and sVCAM-1. In contrast, when CD8 T_{ang} cells were TCR stimulated a significant
528 increase of sICAM-1 and sVCAM-1 was detected in the supernatant of the cultures (Figure 5A).
529 The effects mediated by CD8 T_{ang} cells from PWH were significantly higher than those observed
530 with CD8 T_{ang} cells from PWoH (Figure 5A). Moreover, stimulation of CD8 T_{ang} from PWH led
531 to an increased trend, although did not reach statistical significance, in the production of pro-
532 inflammatory and pro-angiogenic cytokines IL-6, and bFGF respectively. No differences were
533 observed in the secretion of IL-8 Angiopoietin-2 (Ang-2) and VEGF. (Figure 5B). The
534 combination of cytokines IFNγ (10 ng/mL) and TNFα (0.5 ng/mL) used as positive control in
535 HUVEC cultured alone, showed no statistically significant effect on the shedding of sVCAM-1,

536 sICAM-1. In addition, low IL-6 secretion was observed suggesting that CD8 T_{ang} cell-HUVEC
537 contact dependent mechanism is involved in mediating shedding of adhesion molecules and IL-6
538 secretion by endothelial cells (Figure S6B and Figure 5B). Similar levels of Ang-2, IL-8/CXCL8
539 and the pro-angiogenic cytokines VEGF and FGFb were detected when endothelial cells were
540 stimulated with combination IFNγ and TNFα (Figure S6B).

541 These observations suggest that secretion of cytokines and effector molecules from activated
542 CD8 T_{ang} cells can lead to endothelial activation promoting trafficking of immune cells and
543 secretion of pro-inflammatory and pro-angiogenic cytokines by endothelial cells.

544 We next performed a tube forming assay in which endothelial cells cultured in an extracellular
545 matrix form capillary-like structures as a measurement of angiogenesis to better evaluate the
546 interactions between CD8 T_{ang}-endothelial cells (92). CD8 T_{angs} cells were sorted from PBMCs,
547 labeled with CFSE and cultured with HUVEC at 1:2 T cell to HUVEC ratio (Figure 5C and D).

548 CD8 T_{ang} cells overtime migrate and adhere to the endothelial cells as the tubes formed
549 showing a mesh of capillary-like structures and $CFSE^{+}$CD8 T_{ang}, suggesting a close interaction
550 with endothelial cells in the extracellular matrix (Figure 5C and D). Overtime, $CSFE^{+}$CD8 T_{ang}
551 from PWH and sorted HIV_{Gag} specific CD8 T cells showed a trend of slowing the growth of the
552 tube (loop area), although these responses were heterogenous among the donors (Figure 5E). In
553 contrast, CD8 T_{ang} from PWoH showed a trend promoting bigger loop area overtime.

554 Altogether, these data imply a cross-talk between CD8 T_{ang} cells and endothelial cells. CD8
555 T_{ang} cells from PWH promote endothelial activation (ICAM1 and VCAM1), and induced secretion
556 of pro-inflammatory and pro-angiogenic cytokines influencing endothelial cell function.

557

558 **Activated CD8 T_{ang} cells mediate endothelial cell activation through a granzyme-**
559 **dependent PAR1 activation**

560 We next investigated the mechanisms by which CD8 T_{ang} cells activate endothelial cells.
561 PAR1 is expressed by endothelial cells and its signaling mediates important functions in
562 maintaining barrier function (32). In addition, PAR1 connects endothelial cells and CD8 T cells at
563 the site of vascular injury (38, 40, 41). The above data shows that CD8 T_{ang} cells express PAR1
564 and endothelial homing markers, and $GZMA^{+}GZMB^{+}$CD8 T_{ang} cells are associated with ASCVD
565 (Figure 4). These observations and the evidence that in addition to thrombin, other proteases
566 including granzymes (A, B and K) activate PAR1, led us to the hypothesis that granzymes are
567 involved in endothelial activation in the context of HIV infection (93-95).

568 GZMs were first thought to be mainly involved in cytotoxic function, however non-cytotoxic
569 and extracellular biological activities including regulation of vascular integrity, angiogenesis,
570 extracellular matrix remodeling have been reported (93, 96, 97). In contrast to thrombin,
571 granzymes cleavage site and the downstream signaling pathways differ from thrombin leading to
572 a non-canonical activation of PAR1 called biased signal (43-50, 98, 99).

573 We next studied the effects of granzymes in endothelial cells. To isolate the effects of
574 granzymes from cytokines secreted by CD8 T_{ang} cells we used recombinant human (rh) GZMA
575 and GZMK. GZMA and GZMK have tryptase activity and preferentially cleave after basic
576 residues (Arg and Lys) which is similar to thrombin. GZMB is an aspartase and cleaves after Asp
577 (49, 50, 98, 99).

578 We determined the effects of GZs dependent PAR1 activation on calcium mobilization.
579 HUVEC were cultured *in vitro* and activated either with rhGZMA (100nM) and Thrombin (3nM).
580 Compared to thrombin, GZMA induced a calcium mobilization with slower kinetics and sustained

581 overtime (Figure 6B). These effects were not observed on GZMK and GZMB (data not shown).
582 We then investigated the downstream effects induced by GZM-dependent activation of PAR1 at
583 later time points of stimulation and measure cytokine secretion by endothelial cells (Figure 6C).

584 HUVEC were activated with either rhGZMA and rhGZMK (100 nM) in the absence or
585 presence of PAR1 antagonist SCH530348 which inhibit binding of the tethered ligand (Figure 6A).
586 In addition, we used the mAb ATAP-2 that blocks PAR1 cleavage by binding to an epitope within
587 the PAR1 tethered ligand domain, Figure 6A (43, 100-102). As positive control, we used an agonist
588 peptide specific for PAR1 (mimics the tethered ligand) and mediates activation of PAR1 in a
589 cleavage independent manner (Figure 6A).

590 We found that rhGZMA and rhGZMK induced secretion of pro-inflammatory cytokines IL-
591 6, IL-8/CXCL8 and Ang-2 (Figure 6 and Figure S6C). Moreover, GZA and GZK induced pro-
592 angiogenic cytokine VEGF, albeit at lower levels (Figure S7). The antagonist SCH530348
593 (vorapaxar) partially blocked PAR1 activation by rhGZMA and consequently the secretion of IL-
594 6 and IL-8 and Ang-2 (Figure 6C, D and E). The effects mediated by the ATAP-2 mAb showed
595 inhibition Ang-2 but not IL-6 and IL-8.

596 In addition, rhGZMK dependent PAR1 activation by the antagonist SCH530348 inhibited
597 secretion of IL-6 and IL-8/CXCL8 but not Ang-2 secretion by endothelial cells (Figure 6C, D and
598 E). In contrast, ATAP-2 mAb blocked GZMK dependent PAR1 activation and the secretion of
599 IL-6, IL-8/CXCL8 and Ang-2 (Figure 6C and S7). As expected, stimulation with PAR1 agonist
600 peptide (cleavage independent activation) induced secretion of IL-6 and IL-8, however it did not
601 induce a significant increase in secretion of Ang-2 (Figure 6H and S6C).

602 All together these data suggest that CD8 T_{ang} cells mediate endothelial cell activation in part
603 through GZMA and GZMK dependent PAR1 activation leading to the secretion of pro-
604 inflammatory cytokines.
605

606 **Discussion**

607 Chronic CD8 T cell activation is associated with increased cardiovascular disease risk in PWH,
608 however the mechanisms remain to be defined (10, 11, 18, 22, 23). Because endothelial
609 inflammation and dysfunction are the main features of cardiovascular disease, in the present study
610 we investigated a physiological mechanism in which the immune system (with a focus on CD8 T
611 cells) intersects with the homeostasis of the endothelium such as the vascular repair mechanism in
612 the setting of a systemic viral infection.

613 In this study, using a PAR1 reporter mouse we established the dynamics of PAR1 expression
614 in virus-specific CD8 T cells during the course of an acute viral infection with LCMV. We showed
615 that PAR1 expression in LCMV-specific CD8 T cells is downregulated during the effector phase
616 and its expression is upregulated during the contraction phase and early memory development (day
617 21 p.i). In addition, we determined that a subset of CD8 T cells expressing $CD31^{high}$ play a role
618 endothelial repair providing new evidence of the important role of CD8 T_{ang} cells in vascular repair
619 and remodeling in the setting of a viral infection.

620 T_{ang} cells were originally discovered in the center of endothelial progenitor cell colonies from
621 PBMCs by Hur J. et al. (26). Vascular repair is mediated in part by T_{ang} cells that support
622 proliferation and differentiation of bone marrow derived and resident endothelial progenitor
623 cells/endothelial colony forming cells (EPC/ECFC) at the site of injury (26-28). However, the
624 type CD4 and CD8 of T cells involved in angiogenic function and whether they are virus-specific
625 T cells in the setting of infection has not been elucidated.

626 In the present study, we investigated endothelial injury and repair during acute LCMV
627 infection. We found that expansion of $CD31^{high}$CD8 T cells occurs concomitant with the EC
628 recovery and TCR stimulation of $CD31^{high}$CD8 T cells showed secretion of pro-angiogenic

629 cytokines VEGF and GMCSF. These cytokines are associated with endothelial cell proliferation,
630 survival and bone marrow mobilization of endothelial progenitors (67-69, 103). Accordantly,
631 previous reports showed that administration of GMCSF and granulocyte colony stimulating factor
632 (G-CSF) induced mobilization of pro-angiogenic cells in patients with acute myocardial infarction
633 (69, 104). Moreover, mobilization endothelial progenitor cells by GMCSF enhanced endothelial
634 regeneration and reduced vascular inflammation after intravascular radiation (105, 106). Our study
635 shows that $CD31^{high}CD8\ T_{ang}$ cells may regulate angiogenesis by promoting the recruitment of
636 endothelial progenitor cells, and other cells including myeloid cells to the site of vascular
637 remodeling as depletion of total CD8 T cells delay the recovery of ECs.

638 Particularly, $CD31^{high}CD8\ T_{ang}$ cells expressed CD309 (VEGFR2) and secrete pro-angiogenic
639 and Th1 cytokines. Similar to these findings, a study reported that hypoxia upregulates expression
640 of CD309 (VEGFR2) and VEGF signaling, which in turn increaseed expression of IFNγ and
641 inhibited IL-10 (68). In our model of a systemic viral infection with LCMV, immune mediated
642 pathology may induce hypoxia driving expression of CD309 and secretion of VEGF by CD8 T_{ang}
643 cells. It is also possible VEGF signal promotes the acquisition of a pro-angiogenic property by
644 CD8 T_{ang} cells and warrants further investigation.

645 CD8 T cells are predominantly viewed as main players in immunity against viruses and cancer
646 due to their cytotoxic function, however, emerging evidence suggest that they play a role in tissue
647 regeneration and remodeling. $CD31^{high}CD8\ T_{ang}$ cells were LCMV-specific and secrete VEGF,
648 IFNγ and TNFα and degranulate upon *in vitro* stimulation LCMVGp33 suggesting that may be a
649 function of memory cells after viral control. More importantly, $CD31^{high}CD8\ T_{ang}$ cells showed a
650 memory precursor phenotype ($KLGRG1^{-}CD127^{+}$) suggesting a survival advantage during the
651 contraction phase and a proliferative potential since they produce IL-2 (63-66).

652 Expression of CD31 in T cells has been associated with T cell trafficking and studies have
653 shown that CD31 attenuates TCR signaling in T cells as contains two immunoreceptor tyrosine-
654 based inhibitory motif (ITIM) units in the cytoplasmic domain (107-109). It is possible that CD31
655 expression in CD8 T_{ang} cells allows close interactions with endothelial cells preventing their
656 potential cytotoxic activity on endothelial cells.

657 CD8 T cells with tissue remodeling properties that secrete IFNγ, TNFα and epidermal growth
658 factor receptor (EGFR)-ligand amphiregulin (AREG) have been described highlighting CD8 T cell
659 function beyond cytotoxicity (110). Moreover, in pathological conditions such as retinal vascular
660 diseases, VEGF producing CD8 T cells drive inflammation and abnormal angiogenesis suggesting
661 that dysregulated T_{ang} cell function may contribute to the pathology of disease (111).

662 We also investigated changes in lung endothelial cells. ECs are heterogenous and play distinct
663 roles during immune response by supporting trafficking of immune cells, immune functions
664 (immune cell-like ECs) and repair (regenerative ECs) (73, 112). Particularly, our study shows that
665 at the peak of CD8 T cell recruitment into the lung, ECs expressed high levels of PD-L1 likely
666 induced by cytokines produced by LCMV-specific CD8 T cells regulating the immune mediated-
667 pathology including endothelial injury (113). The "immune-EC" phenotype returns to basal levels
668 when the virus is controlled and ECs expressing receptors associated with cell proliferation and
669 survival (CD34, CD309, CD105, CD201) are more predominant.

670 Studies of lung endothelial cells in response to acute lung injury by LPS and influenza infection
671 using single cell RNAseq, revealed distinct functions of ECs "immune-ECs" and "regenerative-
672 ECs" the later involved in vascular remodeling suggesting an important cross-talk between ECs,
673 host immunity and endothelial repair (74, 76). In contrast to these studies that used an acute
674 respiratory lung viral infection or injury, we used a systemic virus to evaluate vascular injury and

675 investigate potential mechanisms associated with chronic HIV infection and endothelial
676 inflammation. Similar to our studies, the authors observed a trend of reduced EC count at day 7
677 p.i, (76). Although this study did not investigate the potential mechanisms driving proliferation of
678 ECs in the reconstitution phase (between day 14 to 21 p.i), they described a proliferating
679 population of $CD34^{+}$ECs with regenerative capacity (76). We found that CD8 T_{ang} cells play a role
680 in this phase and are associated with population of ECs (cluster 6) that express CD34 and have the
681 potential to proliferate in response to pro-angiogenic cytokines through CD309 and CD105
682 signaling. CD309, the receptor for VEGF, is a critical factor for endothelial cell proliferation,
683 migration, and survival, and plays important role during vascular remodeling (114). In addition,
684 CD105, a marker for endothelial cell proliferation, is expressed on vascular endothelium during
685 angiogenesis and prevents endothelial cell apoptosis induced by TGFβ (115, 116). Moreover, this
686 EC population express of endothelial protein C receptor (CD201) that has been proposed as a
687 marker of endothelial progenitor cells with new vessel forming properties (83, 117, 118).

688 T_{ang} cells are key players in maintaining endothelial homeostasis and alterations in vascular
689 repair mechanisms may contribute to endothelial dysfunction and increase cardiovascular disease
690 risk (119). In fact, reduced proportion of circulating T_{angs} has been associated with age and
691 increased cardiovascular risk (26, 29, 30). Patients with rheumatoid arthritis and inflammatory
692 diseases that suffered a cardiovascular event complication had lower circulating T_{ang} cells (30, 86,
693 120-124).

694 The role of T_{ang} cells in the setting of chronic viral infections including HIV is largely
695 unknown. HIV-associated T cell immune activation and inflammation drives cardiovascular risk,
696 independently of traditional risk factors, duration of antiretroviral treatment and CD4 counts (1-
697 15, 125-127). In this study, we hypothesized that HIV-driven CD8 T cell immune activation has a

698 detrimental effect on T_{ang} cell function, compromising their ability to promote endothelial repair,
699 and chronic interference of this pathway results in vascular inflammation/damage and increased
700 risk of disease.

701 PAR1 signaling mediates the cross-talk between the coagulation system, endothelium and
702 adaptive immune system (CD8 T cells) (38-41). We found that compared with uninfected controls
703 (PWoH), CD8 T_{ang} cells from PWH had pro-inflammatory phenotype, express PAR1, and the
704 adhesion and homing receptors CD49f and CX3CR1 respectively (39, 87, 128). In addition, CD8
705 T_{ang} cells had cytotoxic potential and expressed GZMA and GZMB. The activated phenotype of
706 CD8 T_{ang} cells but not CD4 T_{ang} was associated with the ASCVD suggesting a relationship between
707 endothelial inflammation and CD8 T_{ang} cell immune activation.

708 PAR1 is the main receptor of thrombin, however, other serine proteases including granzymes
709 activate PAR1 promoting inflammation (44, 47, 50, 129-131). Granzymes (GZMA, GZMB,
710 GZMK), can activate PAR1 and induce a "biased" or non-canonical signal distinct from thrombin
711 (93-95). GZMs were first thought to be involved in cytotoxic function and recent evidence
712 suggests non-cytotoxic and extracellular biological activities including regulation of vascular
713 integrity, angiogenesis, extracellular matrix remodeling and trans-endothelial migration (32, 46-
714 48, 50, 93, 94, 96, 97, 132). The present study shows that, *in vitro*, CD8 T_{ang} cells induced
715 activation of ECs via granzyme induced production of pro-inflammatory cytokines. In addition,
716 granzyme dependent PAR1 activation provides a potential mechanism by which HIV alters pro-
717 angiogenic function and the chronic stimulation of this pathway may lead endothelial
718 inflammation and dysfunction.

719 Granzymes are emerging as potential contributors of inflammation in cardiovascular diseases
720 (93, 94, 133-136). Recent study reported a subset of CD8 T cells expression GZMK and GZMB

721 with proinflammatory (rather than cytotoxic) function in chronically inflamed human tissues
722 supporting their potential role in inflammation (97). Moreoever, increased levels of GZMs in
723 biological fluids and tissues has been reported in inflammatory conditions including cardiovascular
724 disease, autoimmunity, chronic obstructive pulmonary disease, and cancer (20, 93, 97, 134, 135,
725 137-146). Supporting these observations, we found an association between plasma GZMA leves
726 and endothelial inflammation markers including sVCAM1 and IL-6 was observed in PWH
727 suggesting that ongoing endothelial inflammation in the setting of suppressed viremia may be
728 driven by T_{ang} cell activation.

729 Alltoghether these data highlight a novel role of CD8 T_{ang} cells in vascular remodeling, and
730 granzyme-PAR1 dependent pathway promoting endothelial inglammation. CD8 T_{ang} cells and
731 GZMA dependent PAR1 activation could be a target of intervetion to reduce endothelial
732 inflammation and injury in PWH potentially mitigating the risk of cardiovascular disease during
733 chronic HIV infection.

Acknowledgements

Research reported in this publication was supported by the National Institute of Allergy and Infectious Diseases of the National Institutes of Health under award number NIH R01AI145549 and R21AI186960. We thank the District of Columbia Center for AIDS Research, an NIH funded program (P30AI117970) which is supported by the following NIH Co-Funding and Participating Institutes and Centers: NIAID, NCI, NICHD, NHLBI, NIDA, NIMH, NIA, NIDDK, NIMHD, NIDCR, NINR, FIC and OAR. The content of this publication does not necessarily reflect the views or policies of the Department of Health and Human Services, nor does mention of trade names, commercial products, or organizations imply endorsement by the U.S. Government.

Authors' contributions

MC conceptualized the study and supervise data analysis. TL, CM, CJ performed and analyzed mice experiments, JC, ZZ, MFC, MA, SY, performed human experiments, JK, PK, HC recruited patients, KDV, GPA advise and performed endothelial assay, DBG and LP advice mice infection model. MC, TL and LP wrote the manuscript.

750 **References**

751 1. Baker JV, Sharma S, Grund B, Rupert A, Metcalf JA, Schechter M, et al. Systemic
752 Inflammation, Coagulation, and Clinical Risk in the START Trial. *Open Forum Infect*
753 *Dis.* 2017;4(4):ofx262.
754 2. Molina JM, Grund B, Gordin F, Williams I, Schechter M, Losso M, et al. Which HIV-
755 infected adults with high CD4 T-cell counts benefit most from immediate initiation of
756 antiretroviral therapy? A post-hoc subgroup analysis of the START trial. *Lancet HIV.*
757 2018.
758 3. Hadigan C, Paules CI, and Fauci AS. Association Between Human Immunodeficiency
759 Virus Infection and Cardiovascular Diseases: Finding a Solution to Double Jeopardy.
760 *JAMA Cardiol.* 2017;2(2):123-4.
761 4. Hsue PY, Deeks SG, and Hunt PW. Immunologic basis of cardiovascular disease in HIV-
762 infected adults. *The Journal of infectious diseases.* 2012;205 Suppl 3:S375-82.
763 5. Sinha A, Ma Y, Scherzer R, Hur S, Li D, Ganz P, et al. Role of T-Cell Dysfunction,
764 Inflammation, and Coagulation in Microvascular Disease in HIV. *Journal of the*
765 *American Heart Association.* 2016;5(12).
766 6. Lipshultz SE, Miller TL, Wilkinson JD, Scott GB, Somarriba G, Cochran TR, et al.
767 Cardiac effects in perinatally HIV-infected and HIV-exposed but uninfected children and
768 adolescents: a view from the United States of America. *J Int AIDS Soc.* 2013;16:18597.
769 7. Miller TL, Somarriba G, Orav EJ, Mendez AJ, Neri D, Schaefer N, et al. Biomarkers of
770 vascular dysfunction in children infected with human immunodeficiency virus-1. *J*
771 *Acquir Immune Defic Syndr.* 2010;55(2):182-8.
772 8. Grund B, Baker JV, Deeks SG, Wolfson J, Wentworth D, Cozzi-Lepri A, et al. Relevance
773 of Interleukin-6 and D-Dimer for Serious Non-AIDS Morbidity and Death among HIV-
774 Positive Adults on Suppressive Antiretroviral Therapy. *PLoS One.* 2016;11(5):e0155100.
775 9. Freiberg MS, Chang CC, Kuller LH, Skanderson M, Lowy E, Kraemer KL, et al. HIV
776 infection and the risk of acute myocardial infarction. *JAMA internal medicine.*
777 2013;173(8):614-22.
778 10. Longenecker CT, Funderburg NT, Jiang Y, Debanne S, Storer N, Labbato DE, et al.
779 Markers of inflammation and CD8 T-cell activation, but not monocyte activation, are
780 associated with subclinical carotid artery disease in HIV-infected individuals. *HIV Med.*
781 2013;14(6):385-90.
782 11. Mattingly AS, Unsal AB, Purdy JB, Gharib AM, Rupert A, Kovacs JA, et al. T-cell
783 Activation and E-selectin Are Associated With Coronary Plaque in HIV-infected Young
784 Adults. *Pediatr Infect Dis J.* 2017;36(1):63-5.
785 12. Serrano-Villar S, Sainz T, Lee SA, Hunt PW, Sinclair E, Shacklett BL, et al. HIV-
786 infected individuals with low CD4/CD8 ratio despite effective antiretroviral therapy
787 exhibit altered T cell subsets, heightened CD8+ T cell activation, and increased risk of
788 non-AIDS morbidity and mortality. *PLoS Pathog.* 2014;10(5):e1004078.
789 13. Stein JH, and Hsue PY. Inflammation, immune activation, and CVD risk in individuals
790 with HIV infection. *JAMA.* 2012;308(4):405-6.
791 14. Longenecker CT, Sullivan C, and Baker JV. Immune activation and cardiovascular
792 disease in chronic HIV infection. *Curr Opin HIV AIDS.* 2016;11(2):216-25.
793 15. Gharib AM, and Hadigan C. Imaging to End Points: Cardiovascular Disease Risk
794 Assessment in HIV. *Circulation Cardiovascular imaging.* 2017;10(10).

795 16. Shah ASV, Stelzle D, Lee KK, Beck EJ, Alam S, Clifford S, et al. Global Burden of
796 Atherosclerotic Cardiovascular Disease in People Living with the Human
797 Immunodeficiency Virus: A Systematic Review and Meta-Analysis. *Circulation.* 2018.
798 17. Triant VA, Perez J, Regan S, Massaro JM, Meigs JB, Grinspoon SK, et al.
799 Cardiovascular Risk Prediction Functions Underestimate Risk in HIV Infection.
800 *Circulation.* 2018;137(21):2203-14.
801 18. Shah ASV, Stelzle D, Lee KK, Beck EJ, Alam S, Clifford S, et al. Global Burden of
802 Atherosclerotic Cardiovascular Disease in People Living With HIV: Systematic Review
803 and Meta-Analysis. *Circulation.* 2018;138(11):1100-12.
804 19. Lundgren JD, Babiker AG, Sharma S, Grund B, Phillips AN, Matthews G, et al. Long-
805 Term Benefits from Early Antiretroviral Therapy Initiation in HIV Infection. *NEJM Evid.*
806 2023;2(3).
807 20. Schafer S, and Zernecke A. CD8(+) T Cells in Atherosclerosis. *Cells.* 2020;10(1).
808 21. Hsue PY, Deeks SG, and Hunt PW. Immunologic basis of cardiovascular disease in HIV-
809 infected adults. *The Journal of infectious diseases.* 2012;205 Suppl 3(Suppl 3):S375-82.
810 22. Kaplan RC, Sinclair E, Landay AL, Lurain N, Sharrett AR, Gange SJ, et al. T cell
811 activation and senescence predict subclinical carotid artery disease in HIV-infected
812 women. *The Journal of infectious diseases.* 2011;203(4):452-63.
813 23. Karim R, Mack WJ, Kono N, Tien PC, Anastos K, Lazar J, et al. T-cell activation, both
814 pre- and post-HAART levels, correlates with carotid artery stiffness over 6.5 years
815 among HIV-infected women in the WIHS. *J Acquir Immune Defic Syndr.*
816 2014;67(3):349-56.
817 24. Keller TT, Mairuhu AT, de Kruif MD, Klein SK, Gerdes VE, ten Cate H, et al. Infections
818 and endothelial cells. *Cardiovascular research.* 2003;60(1):40-8.
819 25. Wang Y, Brichacek B, Dubrovsky L, Pushkarsky T, Korolowicz K, Rodriguez O, et al.
820 Increased atherosclerosis in HIV-infected humanized mice is caused by a single viral
821 protein, Nef. *The Journal of infectious diseases.* 2025.
822 26. Hur J, Yang HM, Yoon CH, Lee CS, Park KW, Kim JH, et al. Identification of a novel
823 role of T cells in postnatal vasculogenesis: characterization of endothelial progenitor cell
824 colonies. *Circulation.* 2007;116(15):1671-82.
825 27. Asahara T, Murohara T, Sullivan A, Silver M, van der Zee R, Li T, et al. Isolation of
826 putative progenitor endothelial cells for angiogenesis. *Science (New York, NY.*
827 1997;275(5302):964-7.
828 28. Yoder MC. Endothelial stem and progenitor cells (stem cells): (2017 Grover Conference
829 Series). *Pulm Circ.* 2018;8(1):2045893217743950.
830 29. Rouhl RP, Mertens AE, van Oostenbrugge RJ, Damoiseaux JG, Debrus-Palmans LL,
831 Henskens LH, et al. Angiogenic T-cells and putative endothelial progenitor cells in
832 hypertension-related cerebral small vessel disease. *Stroke; a journal of cerebral*
833 *circulation.* 2012;43(1):256-8.
834 30. Rodriguez-Carrio J, Alperi-Lopez M, Lopez P, Alonso-Castro S, Ballina-Garcia FJ, and
835 Suarez A. Angiogenic T cells are decreased in rheumatoid arthritis patients. *Ann Rheum*
836 *Dis.* 2015;74(5):921-7.
837 31. Coughlin SR. How the protease thrombin talks to cells. *Proceedings of the National*
838 *Academy of Sciences of the United States of America.* 1999;96(20):11023-7.
839 32. Coughlin SR. Thrombin signalling and protease-activated receptors. *Nature.*
840 2000;407(6801):258-64.

841 33. Soh UJ, Dores MR, Chen B, and Trejo J. Signal transduction by protease-activated
842 receptors. *British journal of pharmacology.* 2010;160(2):191-203.
843 34. Sambrano GR, Weiss EJ, Zheng YW, Huang W, and Coughlin SR. Role of thrombin
844 signalling in platelets in haemostasis and thrombosis. *Nature.* 2001;413(6851):74-8.
845 35. Kahn ML, Zheng YW, Huang W, Bigornia V, Zeng D, Moff S, et al. A dual thrombin
846 receptor system for platelet activation. *Nature.* 1998;394(6694):690-4.
847 36. Ishihara H, Zeng D, Connolly AJ, Tam C, and Coughlin SR. Antibodies to protease-
848 activated receptor 3 inhibit activation of mouse platelets by thrombin. *Blood.*
849 1998;91(11):4152-7.
850 37. Xu WF, Andersen H, Whitmore TE, Presnell SR, Yee DP, Ching A, et al. Cloning and
851 characterization of human protease-activated receptor 4. *Proceedings of the National*
852 *Academy of Sciences of the United States of America.* 1998;95(12):6642-6.
853 38. Green SA, Smith M, Hasley RB, Stephany D, Harned A, Nagashima K, et al. Activated
854 platelet-T-cell conjugates in peripheral blood of patients with HIV infection: coupling
855 coagulation/inflammation and T cells. *AIDS (London, England).* 2015;29(11):1297-308.
856 39. Mudd JC, Panigrahi S, Kyi B, Moon SH, Manion MM, Younes SA, et al. Inflammatory
857 Function of CX3CR1+ CD8+ T Cells in Treated HIV Infection Is Modulated by Platelet
858 Interactions. *The Journal of infectious diseases.* 2016;214(12):1808-16.
859 40. Hurley A, Smith M, Karpova T, Hasley RB, Belkina N, Shaw S, et al. Enhanced effector
860 function of CD8(+) T cells from healthy controls and HIV-infected patients occurs
861 through thrombin activation of protease-activated receptor 1. *The Journal of infectious*
862 *diseases.* 2013;207(4):638-50.
863 41. Chen H, Smith M, Herz J, Li T, Hasley R, Le Saout C, et al. The role of protease-
864 activated receptor 1 signaling in CD8 T cell effector functions. *iScience.*
865 2021;24(11):103387.
866 42. Hollenberg MD. PARs in the stars: proteinase-activated receptors and astrocyte function.
867 Focus on "Thrombin (PAR-1)-induced proliferation in astrocytes via MAPK involves
868 multiple signaling pathways". *American journal of physiology Cell physiology.*
869 2002;283(5):C1347-50.
870 43. Ramachandran R, Noorbakhsh F, Defea K, and Hollenberg MD. Targeting proteinase-
871 activated receptors: therapeutic potential and challenges. *Nature reviews Drug discovery.*
872 2012;11(1):69-86.
873 44. Wang T, Lee MH, Choi E, Pardo-Villamizar CA, Lee SB, Yang IH, et al. Granzyme B-
874 induced neurotoxicity is mediated via activation of PAR-1 receptor and Kv1.3 channel.
875 *PLoS One.* 2012;7(8):e43950.
876 45. Zhao P, Metcalf M, and Bunnett NW. Biased signaling of protease-activated receptors.
877 *Frontiers in endocrinology.* 2014;5:67.
878 46. Lee PR, Johnson TP, Gnanapavan S, Giovannoni G, Wang T, Steiner JP, et al. Protease-
879 activated receptor-1 activation by granzyme B causes neurotoxicity that is augmented by
880 interleukin-1beta. *J Neuroinflammation.* 2017;14(1):131.
881 47. Cooper DM, Pechkovsky DV, Hackett TL, Knight DA, and Granville DJ. Granzyme K
882 activates protease-activated receptor-1. *PLoS One.* 2011;6(6):e21484.
883 48. Sharma M, Merkulova Y, Raithatha S, Parkinson LG, Shen Y, Cooper D, et al.
884 Extracellular granzyme K mediates endothelial activation through the cleavage of
885 protease-activated receptor-1. *The FEBS journal.* 2016;283(9):1734-47.

886 49. Bovenschen N, Quadir R, van den Berg AL, Brenkman AB, Vandenberghe I, Devreese
887 B, et al. Granzyme K displays highly restricted substrate specificity that only partially
888 overlaps with granzyme A. *J Biol Chem.* 2009;284(6):3504-12.
889 50. Suidan HS, Bouvier J, Schaerer E, Stone SR, Monard D, and Tschopp J. Granzyme A
890 released upon stimulation of cytotoxic T lymphocytes activates the thrombin receptor on
891 neuronal cells and astrocytes. *Proc Natl Acad Sci U S A.* 1994;91(17):8112-6.
892 51. Kaiserman D, Zhao P, Rowe CL, Leong A, Barlow N, Joeckel LT, et al. Granzyme K
893 initiates IL-6 and IL-8 release from epithelial cells by activating protease-activated
894 receptor 2. *PLoS One.* 2022;17(7):e0270584.
895 52. !!! INVALID CITATION !!! (52).
896 53. Harker JA, Wong KA, Dallari S, Bao P, Dolgoter A, Jo Y, et al. Interleukin-27R
897 Signaling Mediates Early Viral Containment and Impacts Innate and Adaptive Immunity
898 after Chronic Lymphocytic Choriomeningitis Virus Infection. *Journal of virology.*
899 2018;92(12).
900 54. Haghverdi L, Lun ATL, Morgan MD, and Marioni JC. Batch effects in single-cell RNA-
901 sequencing data are corrected by matching mutual nearest neighbors. *Nat Biotechnol.*
902 2018;36(5):421-7.
903 55. Lopez ML, Soriano-Sarabia N, Bruges G, Marquez ME, Preissner KT, Schmitz ML, et al.
904 Expression pattern of protease activated receptors in lymphoid cells. *Cell Immunol.*
905 2014;288(1-2):47-52.
906 56. Anderson KG, Sung H, Skon CN, Lefrancois L, Deisinger A, Vezys V, et al. Cutting
907 edge: intravascular staining redefines lung CD8 T cell responses. *J Immunol.*
908 2012;189(6):2702-6.
909 57. Masopust D, Vezys V, Marzo AL, and Lefrancois L. Preferential localization of effector
910 memory cells in nonlymphoid tissue. *Science (New York, NY.* 2001;291(5512):2413-7.
911 58. Purton JF, Martin CE, and Surh CD. Enhancing T cell memory: IL-7 as an adjuvant to
912 boost memory T-cell generation. *Immunol Cell Biol.* 2008;86(5):385-6.
913 59. Kang SS, and McGavern DB. Lymphocytic choriomeningitis infection of the central
914 nervous system. *Frontiers in bioscience : a journal and virtual library.* 2008;13:4529-43.
915 60. Baccala R, Welch MJ, Gonzalez-Quintial R, Walsh KB, Teijaro JR, Nguyen A, et al.
916 Type I interferon is a therapeutic target for virus-induced lethal vascular damage.
917 *Proceedings of the National Academy of Sciences of the United States of America.*
918 2014;111(24):8925-30.
919 61. Wherry EJ, Teichgraber V, Becker TC, Masopust D, Kaech SM, Antia R, et al. Lineage
920 relationship and protective immunity of memory CD8 T cell subsets. *Nature*
921 *immunology.* 2003;4(3):225-34.
922 62. Wherry EJ, Blattman JN, Murali-Krishna K, van der Most R, and Ahmed R. Viral
923 persistence alters CD8 T-cell immunodominance and tissue distribution and results in
924 distinct stages of functional impairment. *Journal of virology.* 2003;77(8):4911-27.
925 63. Joshi NS, Cui W, Chandele A, Lee HK, Urso DR, Hagman J, et al. Inflammation directs
926 memory precursor and short-lived effector CD8(+) T cell fates via the graded expression
927 of T-bet transcription factor. *Immunity.* 2007;27(2):281-95.
928 64. Sarkar S, Kalia V, Haining WN, Konieczny BT, Subramaniam S, and Ahmed R.
929 Functional and genomic profiling of effector CD8 T cell subsets with distinct memory
930 fates. *The Journal of experimental medicine.* 2008;205(3):625-40.

931 65. Chang JT, Wherry EJ, and Goldrath AW. Molecular regulation of effector and memory T
932 cell differentiation. *Nature immunology.* 2014;15(12):1104-15.
933 66. Herndler-Brandstetter D, Ishigame H, Shinnakasu R, Plajer V, Stecher C, Zhao J, et al.
934 KLRG1(+) Effector CD8(+) T Cells Lose KLRG1, Differentiate into All Memory T Cell
935 Lineages, and Convey Enhanced Protective Immunity. *Immunity.* 2018;48(4):716-29 e8.
936 67. Perez-Gutierrez L, and Ferrara N. Biology and therapeutic targeting of vascular
937 endothelial growth factor A. *Nat Rev Mol Cell Biol.* 2023;24(11):816-34.
938 68. Mor F, Quintana FJ, and Cohen IR. Angiogenesis-inflammation cross-talk: vascular
939 endothelial growth factor is secreted by activated T cells and induces Th1 polarization. *J*
940 *Immunol.* 2004;172(7):4618-23.
941 69. Wang QR, Wang F, Zhu WB, Lei J, Huang YH, Wang BH, et al. GM-CSF accelerates
942 proliferation of endothelial progenitor cells from murine bone marrow mononuclear cells
943 in vitro. *Cytokine.* 2009;45(3):174-8.
944 70. Bussolino F, Wang JM, Defilippi P, Turrini F, Sanavio F, Edgell CJ, et al. Granulocyte-
945 and granulocyte-macrophage-colony stimulating factors induce human endothelial cells
946 to migrate and proliferate. *Nature.* 1989;337(6206):471-3.
947 71. Biedermann BC. Vascular endothelium: checkpoint for inflammation and immunity.
948 *News in physiological sciences : an international journal of physiology produced jointly*
949 *by the International Union of Physiological Sciences and the American Physiological*
950 *Society.* 2001;16:84-8.
951 72. Danese S, Dejana E, and Fiocchi C. Immune regulation by microvascular endothelial
952 cells: directing innate and adaptive immunity, coagulation, and inflammation. *J Immunol.*
953 2007;178(10):6017-22.
954 73. Amersfoort J, Eelen G, and Carmeliet P. Immunomodulation by endothelial cells -
955 partnering up with the immune system? *Nature reviews.* 2022;22(9):576-88.
956 74. Zhang L, Gao S, White Z, Dai Y, Malik AB, and Rehman J. Single-cell transcriptomic
957 profiling of lung endothelial cells identifies dynamic inflammatory and regenerative
958 subpopulations. *JCI Insight.* 2022;7(11).
959 75. Godoy RS, Cober ND, Cook DP, McCourt E, Deng Y, Wang L, et al. Single-cell
960 transcriptomic atlas of lung microvascular regeneration after targeted endothelial cell
961 ablation. *Elife.* 2023;12.
962 76. Niethamer TK, Stabler CT, Leach JP, Zepp JA, Morley MP, Babu A, et al. Defining the
963 role of pulmonary endothelial cell heterogeneity in the response to acute lung injury.
964 *Elife.* 2020;9.
965 77. Rodor J, Chen SH, Scanlon JP, Monteiro JP, Caudrillier A, Sweta S, et al. Single-cell
966 RNA sequencing profiling of mouse endothelial cells in response to pulmonary arterial
967 hypertension. *Cardiovasc Res.* 2022;118(11):2519-34.
968 78. Jerkic M, Rivas-Elena JV, Prieto M, Carron R, Sanz-Rodriguez F, Perez-Barriocanal F, et
969 al. Endoglin regulates nitric oxide-dependent vasodilatation. *FASEB journal : official*
970 *publication of the Federation of American Societies for Experimental Biology.*
971 2004;18(3):609-11.
972 79. Toporsian M, Gros R, Kabir MG, Vera S, Govindaraju K, Eidelman DH, et al. A role for
973 endoglin in coupling eNOS activity and regulating vascular tone revealed in hereditary
974 hemorrhagic telangiectasia. *Circulation research.* 2005;96(6):684-92.

975 80. Kretschmer S, Dethlefsen I, Hagner-Benes S, Marsh LM, Garn H, and Konig P.
976 Visualization of intrapulmonary lymph vessels in healthy and inflamed murine lung using
977 CD90/Thy-1 as a marker. *PLoS One.* 2013;8(2):e55201.
978 81. Levine JH, Simonds EF, Bendall SC, Davis KL, Amir el AD, Tadmor MD, et al. Data-
979 Driven Phenotypic Dissection of AML Reveals Progenitor-like Cells that Correlate with
980 Prognosis. *Cell.* 2015;162(1):184-97.
981 82. Li Q, Wei S, Li Y, Wu F, Qin X, Li Z, et al. Blocking of programmed cell death-ligand 1
982 (PD-L1) expressed on endothelial cells promoted the recruitment of CD8(+)IFN-
983 gamma(+) T cells in atherosclerosis. *Inflammation research : official journal of the*
984 *European Histamine Research Society [et al].* 2023;72(4):783-96.
985 83. Yu QC, Song W, Wang D, and Zeng YA. Identification of blood vascular endothelial
986 stem cells by the expression of protein C receptor. *Cell research.* 2016;26(10):1079-98.
987 84. Thiyagarajan M, Cheng T, and Zlokovic BV. Endothelial cell protein C receptor: role
988 beyond endothelium? *Circulation research.* 2007;100(2):155-7.
989 85. Zhu Z, Li T, Chen J, Kumar J, Kumar P, Qin J, et al. The Role of Inflammation and
990 Immune Activation on Circulating Endothelial Progenitor Cells in Chronic HIV
991 Infection. *Frontiers in immunology.* 2021;12:663412.
992 86. Kushner EJ, MacEneaney OJ, Morgan RG, Van Engelenburg AM, Van Guilder GP, and
993 DeSouza CA. CD31+ T cells represent a functionally distinct vascular T cell phenotype.
994 *Blood Cells Mol Dis.* 2010;44(2):74-8.
995 87. Pilling JE, Galvin A, Robins AM, Sewell HF, and Mahida YR. Expression of alpha5
996 (CD49e) and alpha6 (CD49f) integrin subunits on T cells in the circulation and the
997 lamina propria of normal and inflammatory bowel disease colonic mucosa. *Scandinavian*
998 *journal of immunology.* 1998;48(4):425-8.
999 88. Gimbrone MA, Jr., and Garcia-Cardena G. Endothelial Cell Dysfunction and the
1000 Pathobiology of Atherosclerosis. *Circulation research.* 2016;118(4):620-36.
1001 89. Singh V, Kaur R, Kumari P, Pasricha C, and Singh R. ICAM-1 and VCAM-1:
1002 Gatekeepers in various inflammatory and cardiovascular disorders. *Clin Chim Acta.*
1003 2023;548:117487.
1004 90. Groten SA, Smit ER, Janssen EFJ, van den Eshof BL, van Alphen FPJ, van der Zwaan C,
1005 et al. Multi-omics delineation of cytokine-induced endothelial inflammatory states.
1006 *Commun Biol.* 2023;6(1):525.
1007 91. Nakamichi M, Akishima-Fukasawa Y, Fujisawa C, Mikami T, Onishi K, and Akasaka Y.
1008 Basic Fibroblast Growth Factor Induces Angiogenic Properties of Fibrocytes to Stimulate
1009 Vascular Formation during Wound Healing. *The American journal of pathology.*
1010 2016;186(12):3203-16.
1011 92. Arnaoutova I, and Kleinman HK. In vitro angiogenesis: endothelial cell tube formation
1012 on gelled basement membrane extract. *Nature protocols.* 2010;5(4):628-35.
1013 93. Zeglinski MR, and Granville DJ. Granzymes in cardiovascular injury and disease.
1014 *Cellular signalling.* 2020;76:109804.
1015 94. Chamberlain CM, and Granville DJ. The role of Granzyme B in atheromatous diseases.
1016 *Canadian journal of physiology and pharmacology.* 2007;85(1):89-95.
1017 95. Choy JC, McDonald PC, Suarez AC, Hung VH, Wilson JE, McManus BM, et al.
1018 Granzyme B in atherosclerosis and transplant vascular disease: association with cell
1019 death and atherosclerotic disease severity. *Modern pathology : an official journal of the*
1020 *United States and Canadian Academy of Pathology, Inc.* 2003;16(5):460-70.

1021 96. Arias M, Martinez-Lostao L, Santiago L, Ferrandez A, Granville DJ, and Pardo J. The
1022 Untold Story of Granzymes in Oncoimmunology: Novel Opportunities with Old
1023 Acquaintances. *Trends Cancer.* 2017;3(6):407-22.
1024 97. Jonsson AH, Zhang F, Dunlap G, Gomez-Rivas E, Watts GFM, Faust HJ, et al.
1025 Granzyme K(+) CD8 T cells form a core population in inflamed human tissue. *Sci Transl*
1026 *Med.* 2022;14(649):eabo0686.
1027 98. Mahrus S, and Craik CS. Selective chemical functional probes of granzymes A and B
1028 reveal granzyme B is a major effector of natural killer cell-mediated lysis of target cells.
1029 *Chem Biol.* 2005;12(5):567-77.
1030 99. Plasman K, Demol H, Bird PI, Gevaert K, and Van Damme P. Substrate specificities of
1031 the granzyme tryptases A and K. *J Proteome Res.* 2014;13(12):6067-77.
1032 100. Zhang C, Srinivasan Y, Arlow DH, Fung JJ, Palmer D, Zheng Y, et al. High-resolution
1033 crystal structure of human protease-activated receptor 1. *Nature.* 2012;492(7429):387-92.
1034 101. Brass LF, Pizarro S, Ahuja M, Belmonte E, Blanchard N, Stadel JM, et al. Changes in the
1035 structure and function of the human thrombin receptor during receptor activation,
1036 internalization, and recycling. *J Biol Chem.* 1994;269(4):2943-52.
1037 102. O'Brien PJ, Prevost N, Molino M, Hollinger MK, Woolkalis MJ, Woulfe DS, et al.
1038 Thrombin responses in human endothelial cells. Contributions from receptors other than
1039 PAR1 include the transactivation of PAR2 by thrombin-cleaved PAR1. *J Biol Chem.*
1040 2000;275(18):13502-9.
1041 103. Qiu C, Xie Q, Zhang D, Chen Q, Hu J, and Xu L. GM-CSF induces cyclin D1 expression
1042 and proliferation of endothelial progenitor cells via PI3K and MAPK signaling. *Cell*
1043 *Physiol Biochem.* 2014;33(3):784-95.
1044 104. Bruno S, Bussolati B, Scacciatella P, Marra S, Sanavio F, Tarella C, et al. Combined
1045 administration of G-CSF and GM-CSF stimulates monocyte-derived pro-angiogenic cells
1046 in patients with acute myocardial infarction. *Cytokine.* 2006;34(1-2):56-65.
1047 105. Cho HJ, Kim HS, Lee MM, Kim DH, Yang HJ, Hur J, et al. Mobilized endothelial
1048 progenitor cells by granulocyte-macrophage colony-stimulating factor accelerate
1049 reendothelialization and reduce vascular inflammation after intravascular radiation.
1050 *Circulation.* 2003;108(23):2918-25.
1051 106. Stabile E, Kinnaird T, la Sala A, Hanson SK, Watkins C, Campia U, et al. CD8+ T
1052 lymphocytes regulate the arteriogenic response to ischemia by infiltrating the site of
1053 collateral vessel development and recruiting CD4+ mononuclear cells through the
1054 expression of interleukin-16. *Circulation.* 2006;113(1):118-24.
1055 107. Newman PJ. Switched at birth: a new family for PECAM-1. *The Journal of clinical*
1056 *investigation.* 1999;103(1):5-9.
1057 108. Fornasa G, Groyer E, Clement M, Dimitrov J, Compain C, Gaston AT, et al. TCR
1058 stimulation drives cleavage and shedding of the ITIM receptor CD31. *J Immunol.*
1059 2010;184(10):5485-92.
1060 109. Ma L, Mauro C, Cornish GH, Chai JG, Coe D, Fu H, et al. Ig gene-like molecule CD31
1061 plays a nonredundant role in the regulation of T-cell immunity and tolerance.
1062 *Proceedings of the National Academy of Sciences of the United States of America.*
1063 2010;107(45):19461-6.
1064 110. Delacher M, Schmidleithner L, Simon M, Stuve P, Sanderink L, Hotz-Wagenblatt A, et
1065 al. The effector program of human CD8 T cells supports tissue remodeling. *The Journal*
1066 *of experimental medicine.* 2024;221(2).

1067 111. Deliyanti D, Figgett WA, Gebhardt T, Trapani JA, Mackay F, and Wilkinson-Berka JL.
1068 CD8(+) T Cells Promote Pathological Angiogenesis in Ocular Neovascular Disease.
1069 *Arterioscler Thromb Vasc Biol.* 2023;43(4):522-36.
1070 112. Pober JS, and Sessa WC. Evolving functions of endothelial cells in inflammation. *Nature*
1071 *reviews.* 2007;7(10):803-15.
1072 113. Frebel H, Nindl V, Schuepbach RA, Braunschweiler T, Richter K, Vogel J, et al.
1073 Programmed death 1 protects from fatal circulatory failure during systemic virus
1074 infection of mice. *The Journal of experimental medicine.* 2012;209(13):2485-99.
1075 114. Lee C, Kim MJ, Kumar A, Lee HW, Yang Y, and Kim Y. Vascular endothelial growth
1076 factor signaling in health and disease: from molecular mechanisms to therapeutic
1077 perspectives. *Signal Transduct Target Ther.* 2025;10(1):170.
1078 115. Li C, Issa R, Kumar P, Hampson IN, Lopez-Novoa JM, Bernabeu C, et al. CD105
1079 prevents apoptosis in hypoxic endothelial cells. *Journal of cell science.* 2003;116(Pt
1080 13):2677-85.
1081 116. Sharma S, Ehrlich M, Zhang M, Blobe GC, and Henis YI. NRP1 interacts with endoglin
1082 and VEGFR2 to modulate VEGF signaling and endothelial cell sprouting. *Commun Biol.*
1083 2024;7(1):112.
1084 117. Cissy Yu Q, Bai L, Chen Y, Chen Y, Peng G, Wang D, et al. Embryonic vascular
1085 establishment requires protein C receptor-expressing endothelial progenitors.
1086 *Development.* 2022;149(12).
1087 118. Lin Y, Banno K, Gil CH, Myslinski J, Hato T, Shelley WC, et al. Origin, prospective
1088 identification, and function of circulating endothelial colony-forming cells in mice and
1089 humans. *JCI Insight.* 2023;8(5).
1090 119. Weil BR, Kushner EJ, Diehl KJ, Greiner JJ, Stauffer BL, and Desouza CA. CD31+ T
1091 cells, endothelial function and cardiovascular risk. *Heart Lung Circ.* 2011;20(10):659-62.
1092 120. Lopez P, Rodriguez-Carrio J, Martinez-Zapico A, Caminal-Montero L, and Suarez A.
1093 Senescent profile of angiogenic T cells from systemic lupus erythematosus patients. *J*
1094 *Leukoc Biol.* 2016;99(3):405-12.
1095 121. de Boer SA, Reijrink M, Abdulahad WH, Hoekstra ES, Slart R, Heerspink HJL, et al.
1096 Angiogenic T cells are decreased in people with type 2 diabetes mellitus and recruited by
1097 the dipeptidyl peptidase-4 inhibitor Linagliptin: A subanalysis from a randomized,
1098 placebo-controlled trial (RELEASE study). *Diabetes Obes Metab.* 2020;22(7):1220-5.
1099 122. Kul A, Ozturk N, Kurt AK, and Arslan Y. Detection of Angiogenic T Cells and
1100 Endothelial Progenitor Cells in Behcet Disease and Determination of Their Relationship
1101 with Disease Activity. *Life (Basel).* 2023;13(6).
1102 123. Manetti M, Pratesi S, Romano E, Bellando-Randone S, Rosa I, Guiducci S, et al.
1103 Angiogenic T cell expansion correlates with severity of peripheral vascular damage in
1104 systemic sclerosis. *PLoS One.* 2017;12(8):e0183102.
1105 124. Zhang G, Liu Y, Qiu Y, Zhang J, Sun J, Zhou Z, et al. Circulating senescent angiogenic T
1106 cells are linked with endothelial dysfunction and systemic inflammation in hypertension.
1107 *J Hypertens.* 2021;39(5):970-8.
1108 125. Deeks SG, Lewin SR, and Havlir DV. The end of AIDS: HIV infection as a chronic
1109 disease. *Lancet.* 2013;382(9903):1525-33.
1110 126. Triant VA. Cardiovascular disease and HIV infection. *Curr HIV/AIDS Rep.*
1111 2013;10(3):199-206.

1112 127. Nou E, Lo J, and Grinspoon SK. Inflammation, immune activation, and cardiovascular
1113 disease in HIV. *AIDS (London, England)*. 2016;30(10):1495-509.
1114 128. Panigrahi S, Chen B, Fang M, Potashnikova D, Komissarov AA, Lebedeva A, et al.
1115 CX3CL1 and IL-15 Promote CD8 T cell chemoattraction in HIV and in atherosclerosis.
1116 *PLoS Pathog.* 2020;16(9):e1008885.
1117 129. Ossovskaya VS, and Bunnett NW. Protease-activated receptors: contribution to
1118 physiology and disease. *Physiological reviews.* 2004;84(2):579-621.
1119 130. van Eck JA, Shan L, Meeldijk J, Hack CE, and Bovenschen N. A novel proinflammatory
1120 role for granzyme A. *Cell Death Dis.* 2017;8(2):e2630.
1121 131. Wensink AC, Hack CE, and Bovenschen N. Granzymes regulate proinflammatory
1122 cytokine responses. *J Immunol.* 2015;194(2):491-7.
1123 132. Richardson KC, Jung K, Pardo J, Turner CT, and Granville DJ. Noncytotoxic Roles of
1124 Granzymes in Health and Disease. *Physiology (Bethesda).* 2022;37(6):323-48.
1125 133. Ikemoto T, Hojo Y, Kondo H, Takahashi N, Hirose M, Nishimura Y, et al. Plasma
1126 granzyme B as a predicting factor of coronary artery disease--clinical significance in
1127 patients with chronic renal failure. *Journal of cardiology.* 2009;54(3):409-15.
1128 134. Kondo H, Hojo Y, Tsuru R, Nishimura Y, Shimizu H, Takahashi N, et al. Elevation of
1129 plasma granzyme B levels after acute myocardial infarction. *Circulation journal : official*
1130 *journal of the Japanese Circulation Society.* 2009;73(3):503-7.
1131 135. Skjelland M, Michelsen AE, Krohg-Sorensen K, Tennoe B, Dahl A, Bakke S, et al.
1132 Plasma levels of granzyme B are increased in patients with lipid-rich carotid plaques as
1133 determined by echogenicity. *Atherosclerosis.* 2007;195(2):e142-6.
1134 136. Hendel A, Hiebert PR, Boivin WA, Williams SJ, and Granville DJ. Granzymes in age-
1135 related cardiovascular and pulmonary diseases. *Cell death and differentiation.*
1136 2010;17(4):596-606.
1137 137. Xu T, Zhu HX, You X, Ma JF, Li X, Luo PY, et al. Single-cell profiling reveals
1138 pathogenic role and differentiation trajectory of granzyme K+CD8+ T cells in primary
1139 Sjogren's syndrome. *JCI Insight.* 2023;8(8).
1140 138. Tsuru R, Kondo H, Hojo Y, Gama M, Mizuno O, Katsuki T, et al. Increased granzyme B
1141 production from peripheral blood mononuclear cells in patients with acute coronary
1142 syndrome. *Heart.* 2008;94(3):305-10.
1143 139. Hiebert PR, Boivin WA, Abraham T, Pazooki S, Zhao H, and Granville DJ. Granzyme B
1144 contributes to extracellular matrix remodeling and skin aging in apolipoprotein E
1145 knockout mice. *Experimental gerontology.* 2011;46(6):489-99.
1146 140. Hansson GK, Holm J, and Jonasson L. Detection of activated T lymphocytes in the
1147 human atherosclerotic plaque. *The American journal of pathology.* 1989;135(1):169-75.
1148 141. Kyaw T, Winship A, Tay C, Kanellakis P, Hosseini H, Cao A, et al. Cytotoxic and
1149 proinflammatory CD8+ T lymphocytes promote development of vulnerable
1150 atherosclerotic plaques in apoE-deficient mice. *Circulation.* 2013;127(9):1028-39.
1151 142. Cochain C, Koch M, Chaudhari SM, Busch M, Pelisek J, Boon L, et al. CD8+ T Cells
1152 Regulate Monopoiesis and Circulating Ly6C-high Monocyte Levels in Atherosclerosis in
1153 Mice. *Circulation research.* 2015;117(3):244-53.
1154 143. Olofsson PS, Soderstrom LA, Wagsater D, Sheikine Y, Ocaya P, Lang F, et al. CD137 is
1155 expressed in human atherosclerosis and promotes development of plaque inflammation in
1156 hypercholesterolemic mice. *Circulation.* 2008;117(10):1292-301.

1157 144. Kolbus D, Ramos OH, Berg KE, Persson J, Wigren M, Bjorkbacka H, et al. CD8+ T cell
1158 activation predominate early immune responses to hypercholesterolemia in Apoe(-)(/)(-)
1159 mice. *BMC Immunol.* 2010;11:58.
1160 145. Kolbus D, Ljungcrantz I, Andersson L, Hedblad B, Fredrikson GN, Bjorkbacka H, et al.
1161 Association between CD8+ T-cell subsets and cardiovascular disease. *J Intern Med.*
1162 2013;274(1):41-51.
1163 146. Tyrrell DJ, Wragg KM, Chen J, Wang H, Song J, Blin MG, et al. Clonally expanded
1164 memory CD8(+) T cells accumulate in atherosclerotic plaques and are pro-atherogenic in
1165 aged mice. *Nat Aging.* 2023;3(12):1576-90.
1166
1167

1168 **Figure Legends**

1169 **Figure 1. PAR1 expression is modulated in LCMVGp33-specific CD8 T lymphocytes during**
1170 **acute LCMV infection.**

1171 *In vivo* expression of PAR1 in splenic cells from naïve C57BL/6-F2r$^{fl/fl}$ (n= 5) and C57BL/6 (n=
1172 5) mice analyzed by flow cytometry. **(A)** Cells were analyzed after gating on live cells, and singlets
1173 and CD45^{+} lymphocytes. Representative contour plots gating cell types: NK cells (CD3^{-}NK1.1^{+}),
1174 B cells (MHCII^{+}B220^{+}), CD4 (CD3^{+}CD4^{+}) and CD8 T cells (CD3^{+}CD8^{+}). **(B)** Representative
1175 histogram of tdTomato (PAR1) expression in CD4 and CD8 T cells, B cells and NK cells from
1176 C57BL/6 mice (solid grey) and C57BL/6-F2r$^{fl/fl}$ mice (black line). **(C)** Median Fluorescence
1177 Intensity (MFI) of tdTomato expression of total splenic cells from C57BL/6 mice (SP) and B cells,
1178 NK and CD4 and CD8 T cells and NK cells from C57BL/6-F2r$^{fl/fl}$ mice. **(D)** Relative *F2r* mRNA
1179 expression in sorted B cells and purified by magnetic isolation of CD4 and CD8 T cells from
1180 C57BL/6-F2r$^{fl/fl}$ mice (n= 6). **(E)** C57BL/6-F2r$^{fl/fl}$ mice were infected with LCMVArm strain (2 x
1181 10^{5} pfu, i.v). Splenic and lung cells were assessed at day 6 and 21 p.i. by flow cytometry. **(F)**
1182 Representative histogram of tdTomato (tdT) expression in total CD8 T cells from naïve (N) and
1183 infected mice at day 6 and 21 p.i. (solid gray). Overlayed, tdTomato expression in LCMVGp33-
1184 specific CD8 T cells detected by H2-D^{b}LCMVGp33 pentamer staining (red line). **(F)** Median
1185 Fluorescence Intensity (MFI) of tdTomato expression in LCMVGp33-specific CD8 T cells
1186 detected by H2-D^{b}LCMVGp33 pentamer staining. Dashed line represents level expression of total
1187 naïve CD8 T cells. **(G)** Representative plot of lung endothelial cells (EC). After excluding dead
1188 cells and doublets, ECs were gated as CD326^{-}CD45^{-}CD31^{+}. Frequency and cell count of lung
1189 endothelial cells from naïve (N) and infected mice at days 6 and 21 p.i. Frequencies of ECs are

1190 expressed as frequency of total live cells. **(H)** Median Fluorescence Intensity (MFI) of tdTomato
1191 expression in lung ECs from naïve (N) and infected mice (day 6 and day 21p.i.).
1192 The bar graph is represented by box and whisker showing the median value with first and third
1193 quartiles in the box, with whiskers extending to the minimum and maximum values. The data in
1194 line graphs represent mean±SEM in each time point. Data are pooled from three independent
1195 experiments with 5-9 naïve animals (C, E and F) and 8-17 per time point (F and H). Statistical
1196 analysis was performed using non-parametric Mann-Whitney test. P value < 0.05 was considered
1197 significant.
1198
1199 **Figure 2. Angiogenic CD8 T cells promote endothelial recovery during acute viral infection.**
1200 **(A)** Schematic presentation of CD8 T cell depletion. C57BL/6-F2r$^{fl/fl}$ mice were infected with
1201 LCMVArm strain (2 x 10^5 pfu, i.v). At day 15 p.i mice were administered anti-CD8α mAb and
1202 IgG2b isotype for control mice. Frequency and cell count of CD8 T cells at day 21p.i in CD8 T
1203 cell depleted mice and IgG treated control mice assessed by flow cytometry. **(B)** Lung endothelial
1204 cell frequency and count from CD8 T cell depleted and control mice at day 21 p.i. Frequencies of
1205 ECs are expressed as frequency of total live cells. **(C)** Representative contour plot of CD31^{high} and
1206 CD309 expression by lung CD8 T cells from naïve mice and infected mice. Frequency and cell
1207 count of CD31^{high}CD8 T cells from naïve (N) mice and infected mice at day 6 and 21 p.i. **(D)** Lung
1208 CD31^{high} and CD31^{neg} CD8 T cells, representative contour plot of secretion of IFNγ, TNFα
1209 secretion and CD107a upon *in vitro* stimulation with LCMVGp33-44 peptide. DMSO was used as
1210 control. **(E)** Representative contour plot of KLRG1 and CD127 expression by LCMVGp33-
1211 specific CD8 T cells. Frequency of KLRG1$^-$CD127$^+$ (R1), KLRG1$^+$CD127$^+$ (R2) and
1212 KLRG1$^+$CD127$^-$ and KLRG1$^-$CD127$^-$ (R3+R4) LCMVGp33 specific CD8 T cells from lung at

1213 days 6 and 21 p.i.. **(F)** Lung CD31^{high} and CD31^{neg} bulk CD8 T cells were sorted from naïve mice
1214 and infected mice at 21 p.i. and stimulated *in vitro* with anti-CD3 and anti-CD28 mAbs coated
1215 plate for 3 days. Detection of VEGF in the supernatants of the culture. The bar graphs are
1216 represented by box and whisker showing the median value with first and third quartiles in the box,
1217 with whiskers extending to the minimum and maximum values. The data in line graphs represent
1218 mean±SEM in each time point. Data are pooled from two independent experiments with 8 naïve
1219 animals (A and B) and 7-16 per time point (C, D and E). Sorted cells from 3 naïve and 6 infected
1220 mice per time point (G). Statistical analysis was performed using non-parametric Mann-Whitney
1221 test. P value < 0.05 was considered significant.
1222
1223 **Figure 3. CD31^{high}CD8 T cells are associated with endothelial that express a regenerative**
1224 **phenotype.**
1225 **(A)** Unsupervised clustering analysis of lung endothelial cells using phonograph (k= 100). The
1226 heatmap represent mean fluorescence intensity of CD31, PDL1, tdTomato, CD34, CD309,
1227 VCAM-1, CD105, CD90.2 and CD201 expression in ECs. Bubble plots represent the mean
1228 frequency of each cluster from naïve and infected mice at day 6 and 21 p.i. **(B)** Relationship
1229 between frequency of Cluster 6 and lung CD31^{high}CD8 T cells. Data are pooled from two
1230 independent experiments with 7 naïve (A and B) and 8-10 per time point animals (A and B).
1231 Correlation were performed using non-parametric Spearman correlation and p value $\leqslant$ 0.01 was
1232 considered significant.
1233
1234 **Figure 4. Pro-inflammatory phenotype of CD8 T_{ang} correlates to ASCVD risk in PWH.**
1235 Circulating T_{ang} were analyzed in PBMCs from PWH (n= 25, red symbols) and PWoH (n= 17,
1236 blue symbols) by flowcytometry. After gating on live cells and singlets, CD4 and CD8 T cells

1237 were analyzed based on expression of CD31 and CXCR4: **(A)** Representative contour plots for
1238 gating angiogenic T cells, CD4 T_{ang} ($CD31^{+}CXCR4^{+}$) and CD8 T_{ang} ($CD31^{+}CXCR4^{+}$). **(B)**
1239 Frequency of CD4 T_{ang} and CD8 T_{ang} from PWH and PWoH. CD4 T_{ang} and CD8 T_{ang} expression
1240 of: (**C**) CX3CR1 and PAR1 **(D)** CD49f and PAR1 **(E)** granzyme A (GZMA) and B (GZMB). **F,**
1241 **G and H.** Relationship between expression of CD4 and CD8 T_{ang} cells and atherosclerotic
1242 cardiovascular disease (ASCVD) risk score in PWH. **(I)** Relationship between expression of
1243 plasma levels of sVCAM-1, sICAM-1, IL-6 and granzyme A in PWH (n= 25). The bar graph is
1244 represented by box and whisker showing the median value with first and third quartiles in the box,
1245 with whiskers extending to the minimum and maximum values. Statistical analysis was performed
1246 using non-parametric Mann-Whitney test. P value < 0.05 was considered significant. Correlations
1247 were performed using non-parametric Spearman correlation and p value $\leqslant$ 0.01 was considered
1248 significant.
1249
1250 **Figure 5. *In vitro*, CD8 T_{ang} cells from PWH induced shedding of sICAM-1 and sVCAM-1 by**
1251 **endothelial cells.**
1252 CD8 T_{ang} from PWH (n= 10, red symbols) and PWoH (n= 10, blue symbols) were sorted and
1253 stimulated with CD3 and CD28 mAbs coated beads for 3 days and expanded in the presence of
1254 IL-2 for an additional 14 days. Activated CD8 T_{ang} cells were co-cultured with primary human
1255 umbilical vein endothelial cells HUVEC at 2 to 1 CD8 T_{ang} to HUVEC ratio for 24 hours.
1256 Supernatants were collected and measured: **(A)** Soluble vascular cell adhesion molecule 1
1257 (sVCAM1) and intracellular adhesion molecule 1 (sICAM1). **(B)** Cytokines IL-6, Angiopoietin-2
1258 (Ang-2), fibroblast growth factor (bFGF), vascular endothelial growth factor (VEGF) and IL-
1259 8/CXCL8. **(C)** Sorted CD8 T_{ang} memory cells ($CD45RA^{-}CD27^{+}$) from PWH (n= 3, opened red

1260 symbols), PWoH (n= 2, blue symbols), and HIVGag-specific CD8 T cells from PWH (n= 2, solid
1261 red symbols) were labeled with CFSE and cultured with HUVEC at a 2 to 1 ratio in Ibidi chambers
1262 for up to 12 hours. As control, HUVEC were cultured alone (black symbol). Representative phase
1263 contrast images at 2, 4, 6, 8, 10 and 12 hours with masks of tube (black line), branching point
1264 (white point), loop (labeled with number) and CD8 T_{ang} cells (red dots). **(D)** Representative
1265 fluorescent images of T_{ang} cells and HUVEC. **(E)** Fold change of median loop area of individual
1266 donors from PWH and PWoH and HIVGag-specific CD8 T cells. **(F)** Fold change of median loop
1267 area of pooled all donors. HUVEC shows mean±SEM of pooled experiments with all donors. The
1268 bar graph is represented by box and whisker showing the median value with first and third quartiles
1269 in the box, with whiskers extending to the minimum and maximum values. Line graphs represent
1270 the average of all donors. Statistical analysis was performed using non-parametric Mann-Whitney
1271 test. P value < 0.05 was considered significant.
1272
1273 **Figure 6. Activated CD8 T_{ang} cells mediate endothelial cell activation through a granzyme-**
1274 **dependent PAR1 activation**
1275 **(A)** Diagram illustrates the molecular mechanism of cleavage dependent PAR1 activation via
1276 serine proteases. Inhibition of PAR1 activation by ATAP-2 mAb and antagonist SCH530348
1277 (vorapaxar). Peptide agonist (mimics the tethered ligand) and cleavage independent PAR1
1278 activation. The figure was generated with Biorender. **(B)** Image of Granzyme A induced
1279 intracellular calcium mobilization in HUVEC. Intracellular calcium mobilization kinetics in
1280 HUVEC stimulated with granzyme A and thrombin as control. Each line represents the kinetics
1281 overtime of individual cells (lower panel). **(C, D and E)** HUVEC were stimulated with 100 nM of
1282 rh GZMA and GZMK overnight in the presence or absence of 10 μg/mL of ATAP-2 mAb or 300

1283 nM of PAR1 antagonist SCH530348. (**F, G** and **H**) HUVEC were stimulated with 100 μM of
1284 PAR1 agonist peptide (TFLLR-NH2) and peptide control (RLLFT-NH2) as positive and negative
1285 controls respectively. IL-6, IL-8/CXCL8 and Angiopoietin-2 were measured in the supernatants
1286 of the cultures. The bar graph is represented by box and whisker showing the median value with
1287 first and third quartiles in the box, with whiskers extending to the minimum and maximum values.
1288 Statistical analysis was performed using non-parametric Mann-Whitney test. P value <0.05 was
1289 considered significant.
1290

Table 1. Study groups characteristics

Demographics	**PWH (n= 25)**	**PWOH (n= 17)**
Age, yr, median (IQR)	52 (42-57.5)	48 (34-60)
Gender n (%)		
Male	22 (88)	8 (47.1)
Female	3 (12)	9 (52.9)
Ethnicity n (%)		
White	8 (32)	11 (64.8)
African American	12 (48)	3 (17.6)
Other	5 (20)	3 (17.6)
Clinical Characteristics		
Smoker ever, n (%)	8 (32)	N/A
Diabetes, n (%)	9 (36)	N/A
ASCVD risk estimator, median (IQR)[1]	7.9 (5.0-18.6)	N/A
Clinical Laboratory, median (IQR)		
Cholesterol, mg/dL[2]	168 (147-194)	N/A
HDL, mg/dL[3]	47 (41-56.3)	N/A
LDL, mg/dL[3]	99.5 (78.5-117.5)	N/A
HIV Characteristics, median (IQR)		
Viral Load copies/mL[4]	<20 (20-20)	N/A
CD4 count, cells/μL	663 (532-861.5)	N/A
ART treatment		
NRTIs, n (%)	19 (76)	N/A
NNRTIs, n (%)	4 (16)	N/A
PIs, n (%)	4 (16)	N/A
INSTIs, n (%)	14 (56)	N/A
Serum Biomarkers, median (IQR)		
sVCAM-1, pg/mL	288.5 (188.6-366.6)	
IL-6	3.7 (1.2-4.6)	
Granzyme A	256.1 (111.1-514)	
Granzyme B	920.8 (523.4-1566)	
IFNγ	289.8 (87.0-1012)	
TNFα	2.5 (1.1-4.6)	
sFASL	9.8 (3.6-24.1)	

[1] 5 out of 25 participants didn't have ASCVD risk estimator. [2] 10 out of 25 participants didn't have total cholesterol. [3] 11 out of 25 participants didn't have HDL and LDL. [4] 4 out of 25 participants have viral load 110, 70, 60 and 50 HIV RNA copies/mL respectively.

Figure 1

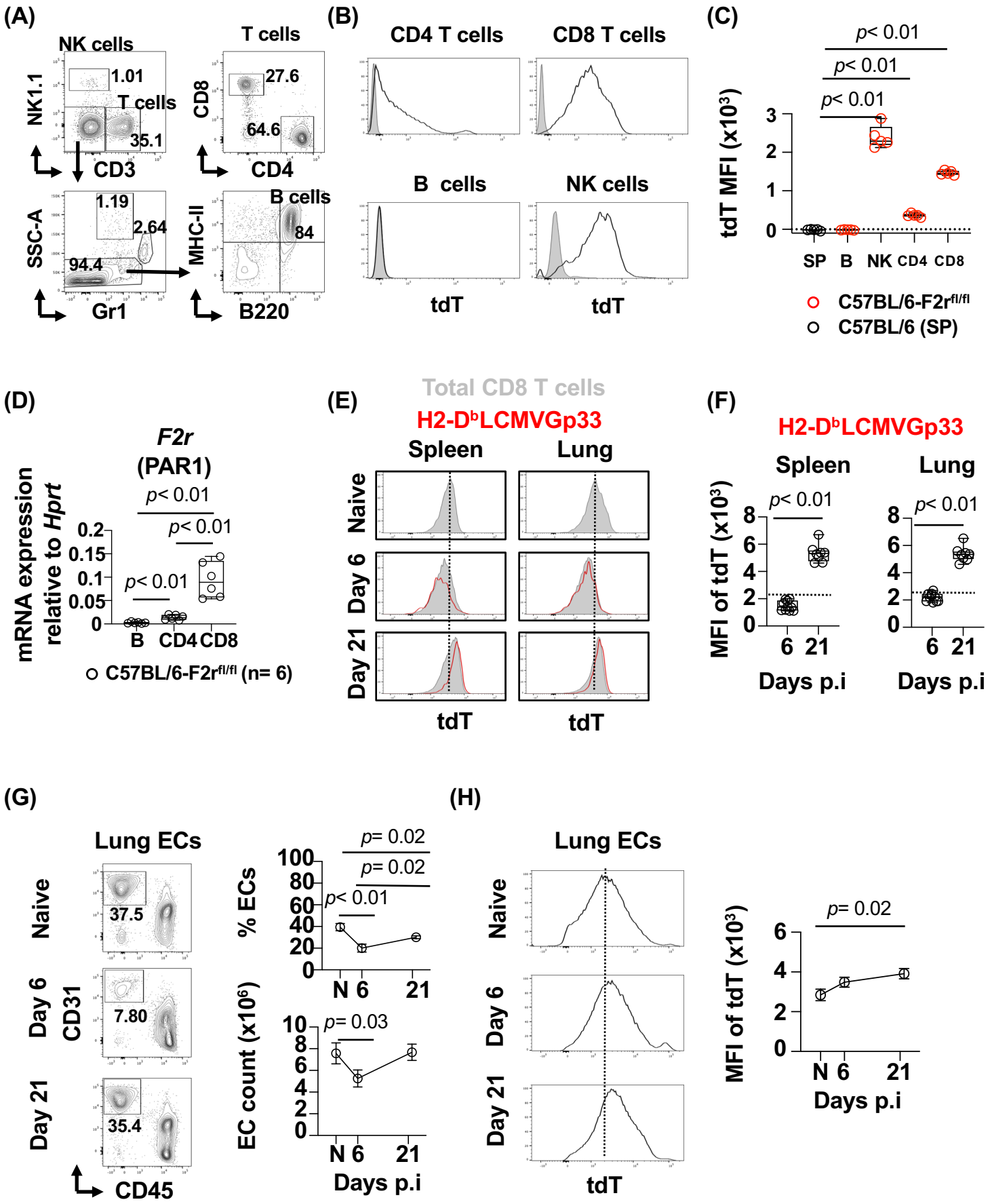
(A)
NK cells
T cells
NK1.1
CD3
1.01
35.1
CD8
CD4
27.6
64.6
SSC-A
Gr1
1.19
2.64
94.4
MHC-II
B220
B cells
84
(B)
CD4 T cells
CD8 T cells
B cells
NK cells
tdT
tdT
(C)
p< 0.01
p< 0.01
p< 0.01
tdT MFI (x10³)
SP B NK CD4 CD8
C57BL/6-F2r fl/fl
C57BL/6 (SP)
(D)
F2r
(PAR1)
mRNA expression relative to Hprt
p< 0.01
p< 0.01
p< 0.01
B CD4 CD8
C57BL/6-F2r fl/fl (n= 6)
(E)
Total CD8 T cells
H2-DbLCMVGp33
Spleen
Lung
Naive
Day 6
Day 21
tdT
tdT
(F)
H2-DbLCMVGp33
Spleen
Lung
MFI of tdT (x10³)
p< 0.01
p< 0.01
6 21
Days p.i
Days p.i
(G)
Lung ECs
Naive
Day 6
Day 21
CD31
CD45
37.5
7.80
35.4
% ECs
p= 0.02
p= 0.02
p< 0.01
N 6 21
EC count (x10⁶)
p= 0.03
N 6 21
Days p.i
(H)
Lung ECs
Naive
Day 6
Day 21
tdT
MFI of tdT (x10³)
p= 0.02
N 6 21
Days p.i

Figure 2

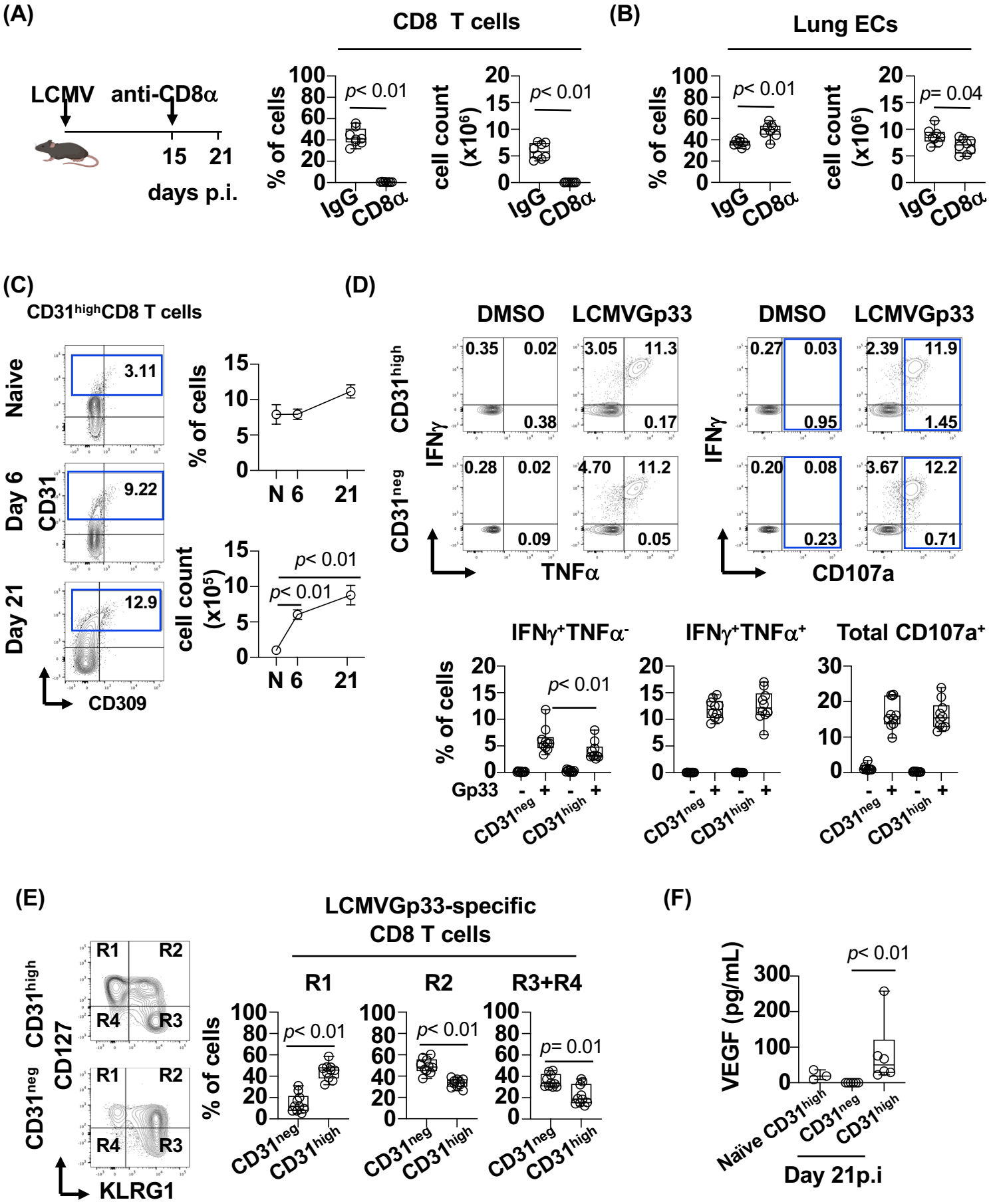
(A)
LCMV
anti-CD8α
15
21
days p.i.
CD8 T cells
% of cells
p< 0.01
IgG
CD8α
cell count (x10^6)
p< 0.01
(B)
Lung ECs
% of cells
p< 0.01
cell count (x10^6)
p= 0.04
(C)
CD31^high CD8 T cells
Naive
Day 6
Day 21
CD31
CD309
3.11
9.22
12.9
% of cells
N 6 21
cell count (x10^5)
p< 0.01
p< 0.01
(D)
DMSO
LCMVGp33
CD31^high
CD31^neg
IFNγ
TNFα
CD107a
0.35 0.02 0.38
3.05 11.3 0.17
0.28 0.02 0.09
4.70 11.2 0.05
0.27 0.03 0.95
2.39 11.9 1.45
0.20 0.08 0.23
3.67 12.2 0.71
IFNγ+TNFα-
IFNγ+TNFα+
Total CD107a+
% of cells
p< 0.01
Gp33
CD31^neg
CD31^high
(E)
LCMVGp33-specific CD8 T cells
CD31^high
CD31^neg
CD127
KLRG1
R1
R2
R3
R4
R1
R2
R3+R4
% of cells
p< 0.01
p< 0.01
p= 0.01
CD31^neg
CD31^high
(F)
VEGF (pg/mL)
p< 0.01
Naïve
CD31^high
CD31^neg
CD31^high
Day 21p.i

Figure 3

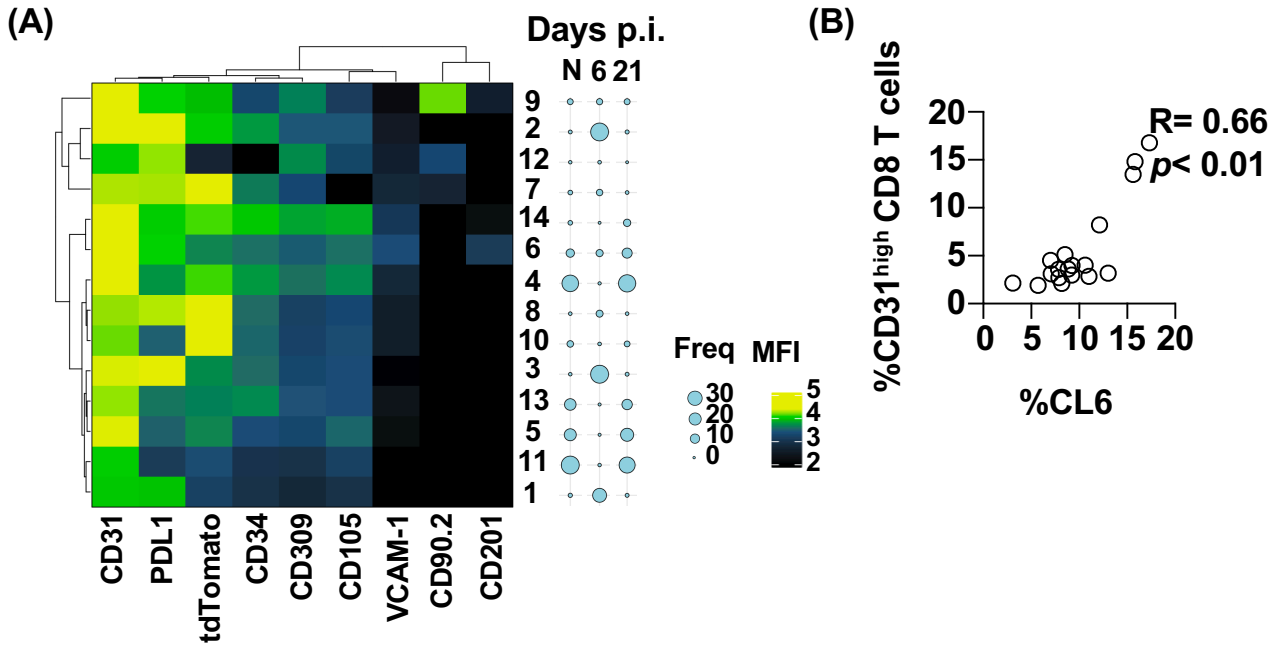
(A)
Days p.i.
N 6 21
9
2
12
7
14
6
4
8
10
3
13
5
11
1
CD31
PDL1
tdTomato
CD34
CD309
CD105
VCAM-1
CD90.2
CD201
Freq
30
20
10
0
MFI
5
4
3
2
(B)
%CD31high CD8 T cells
20
15
10
5
0
0 5 10 15 20
%CL6
R= 0.66
p< 0.01

Figure 4

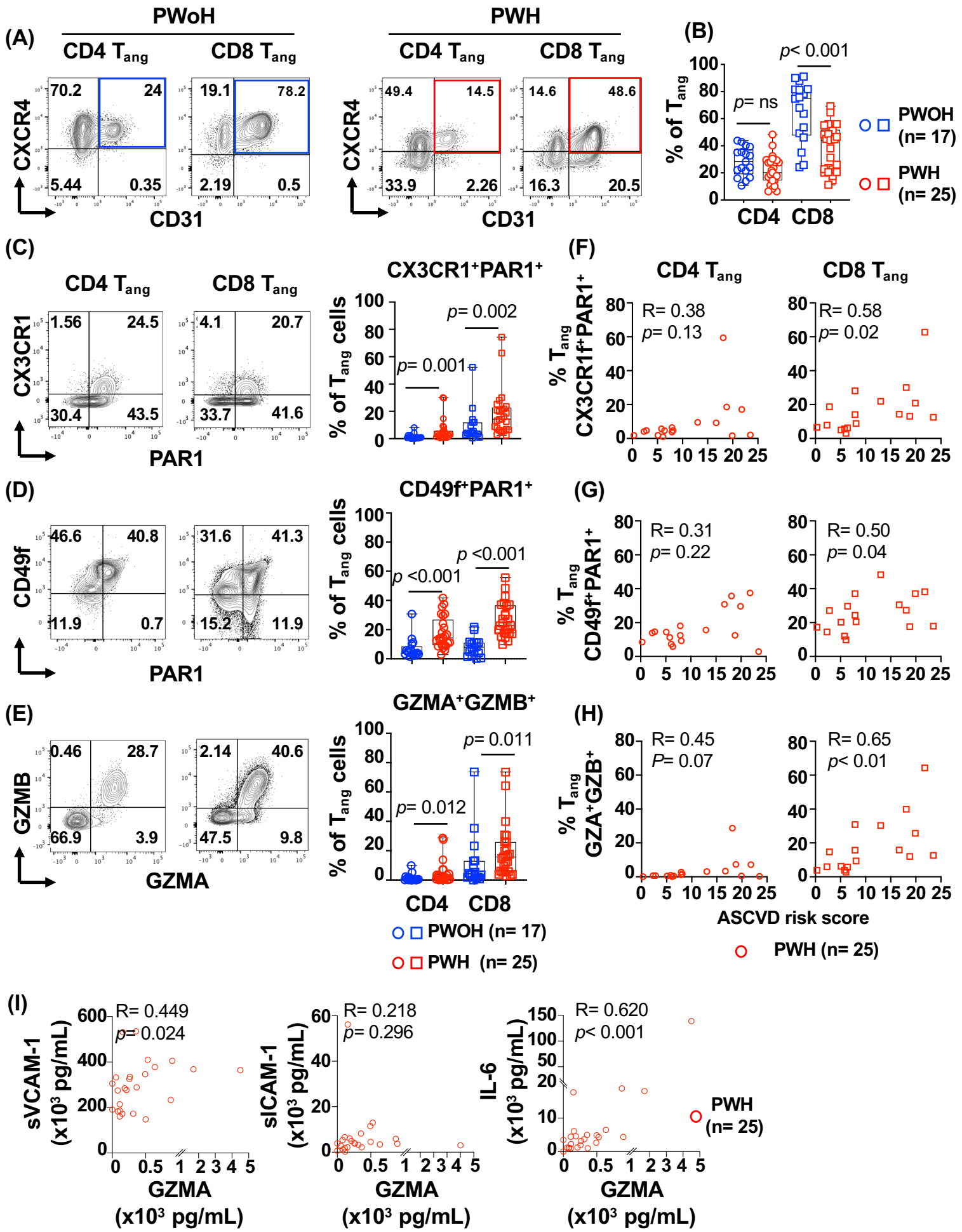
(A)
PWoH
PWH
CD4 Tang
CD8 Tang
CXCR4
CD31
70.2
24
5.44
0.35
19.1
78.2
2.19
0.5
49.4
14.5
33.9
2.26
14.6
48.6
16.3
20.5
(B)
% of Tang
p= ns
p< 0.001
CD4
CD8
PWOH (n= 17)
PWH (n= 25)
(C)
CX3CR1
PAR1
1.56
24.5
30.4
43.5
4.1
20.7
33.7
41.6
CX3CR1+PAR1+
% of Tang cells
p= 0.001
p= 0.002
(D)
CD49f
46.6
40.8
11.9
0.7
31.6
41.3
15.2
11.9
CD49f+PAR1+
p <0.001
p <0.001
(E)
GZMB
GZMA
0.46
28.7
66.9
3.9
2.14
40.6
47.5
9.8
GZMA+GZMB+
p= 0.012
p= 0.011
(F)
CX3CR1f+PAR1+
R= 0.38
p= 0.13
R= 0.58
p= 0.02
(G)
CD49f+PAR1+
R= 0.31
p= 0.22
R= 0.50
p= 0.04
(H)
GZA+GZB+
R= 0.45
P= 0.07
R= 0.65
p< 0.01
ASCVD risk score
(I)
sVCAM-1 (x10³ pg/mL)
R= 0.449
p= 0.024
sICAM-1 (x10³ pg/mL)
R= 0.218
p= 0.296
IL-6 (x10³ pg/mL)
R= 0.620
p< 0.001
GZMA (x10³ pg/mL)
PWH (n= 25)

Figure 5

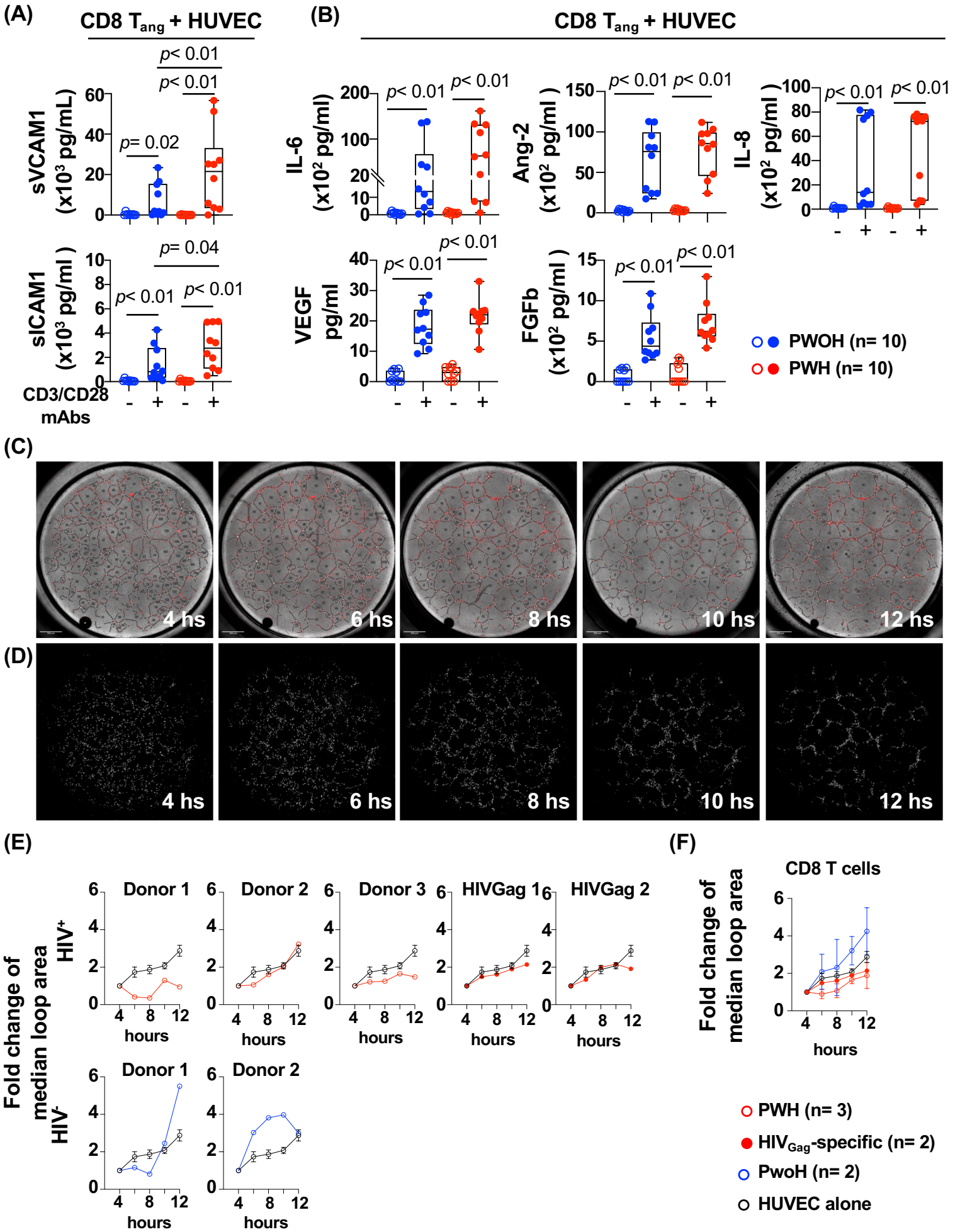
(A)
CD8 Tang + HUVEC
sVCAM1 (x10³ pg/mL)
p= 0.02
p< 0.01
p< 0.01
sICAM1 (x10³ pg/ml)
p< 0.01
p< 0.01
p= 0.04
CD3/CD28 mAbs
(B)
CD8 Tang + HUVEC
IL-6 (x10² pg/ml)
Ang-2 (x10² pg/ml)
IL-8 (x10² pg/ml)
VEGF pg/ml
FGFb (x10² pg/ml)
p< 0.01
PWOH (n= 10)
PWH (n= 10)
(C)
4 hs
6 hs
8 hs
10 hs
12 hs
(D)
4 hs
6 hs
8 hs
10 hs
12 hs
(E)
Fold change of median loop area
HIV+
HIV-
Donor 1
Donor 2
Donor 3
HIVGag 1
HIVGag 2
hours
(F)
CD8 T cells
Fold change of median loop area
hours
PWH (n= 3)
HIVGag-specific (n= 2)
PwoH (n= 2)
HUVEC alone

Figure 6

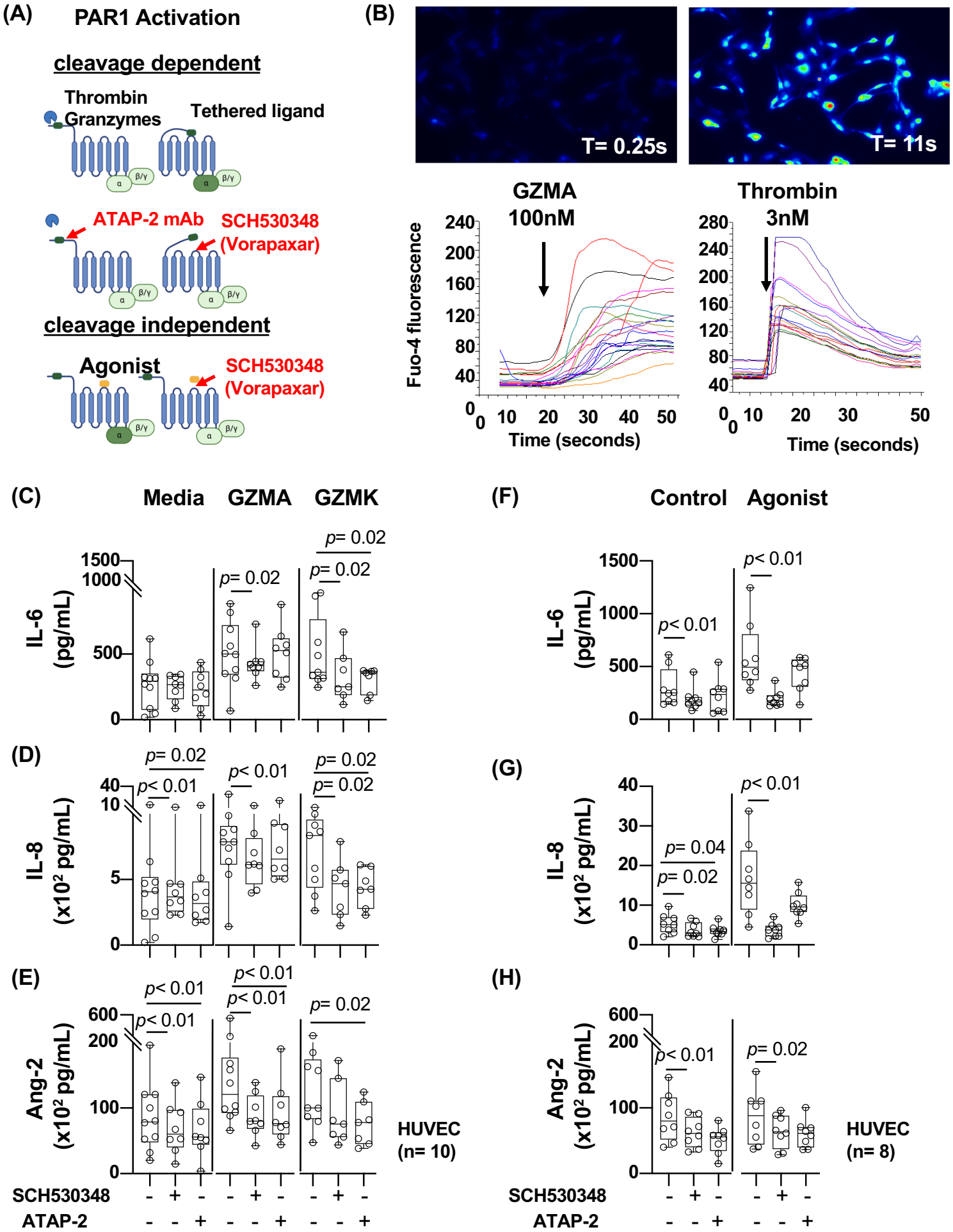
(A)
PAR1 Activation
cleavage dependent
Thrombin
Granzymes
Tethered ligand
ATAP-2 mAb
SCH530348
(Vorapaxar)
cleavage independent
Agonist
SCH530348
(Vorapaxar)
(B)
T= 0.25s
T= 11s
GZMA
100nM
Thrombin
3nM
Fuo-4 fluorescence
Time (seconds)
(C)
Media
GZMA
GZMK
IL-6
(pg/mL)
(D)
IL-8
(x10² pg/mL)
(E)
Ang-2
(x10² pg/mL)
HUVEC
(n= 10)
SCH530348
ATAP-2
(F)
Control
Agonist
(G)
(H)
HUVEC
(n= 8)